Plant, Cell & Environment

Plant, Cell and Environment (2013) **36**, 1547–1563 doi: 10.1111/pce.12091

What does optimization theory actually predict about crown profiles of photosynthetic capacity when models incorporate greater realism?

THOMAS N. BUCKLEY[1], ALESSANDRO CESCATTI[2] & GRAHAM D. FARQUHAR[3]

[1]*Department of Biology, Sonoma State University, Rohnert Park, CA, 94928, USA,* [2]*European Commission, Joint Research Centre, Institute for Environment and Sustainability, Ispra, Italy and* [3]*Research School of Biology, The Australian National University, Canberra, Australia*

ABSTRACT

Measured profiles of photosynthetic capacity in plant crowns typically do not match those of average irradiance: the ratio of capacity to irradiance decreases as irradiance increases. This differs from optimal profiles inferred from simple models. To determine whether this could be explained by omission of physiological or physical details from such models, we performed a series of thought experiments using a new model that included more realism than previous models. We used ray-tracing to simulate irradiance for 8000 leaves in a horizontally uniform canopy. For a subsample of 500 leaves, we simultaneously optimized both nitrogen allocation (among pools representing carboxylation, electron transport and light capture) and stomatal conductance using a transdermally explicit photosynthesis model. Few model features caused the capacity/irradiance ratio to vary systematically with irradiance. However, when leaf absorptance varied as needed to optimize distribution of light-capture N, the capacity/irradiance ratio increased up through the crown – that is, opposite to the observed pattern. This tendency was counteracted by constraints on stomatal or mesophyll conductance, which caused chloroplastic CO_2 concentration to decline systematically with increasing irradiance. Our results suggest that height-related constraints on stomatal conductance can help to reconcile observations with the hypothesis that photosynthetic N is allocated optimally.

Key-words: canopy; nitrogen; photosynthesis; stomata.

INTRODUCTION

Photosynthetic resource allocation in plant crowns has drawn the attention of physiological ecologists for decades. One reason is the importance of allocation in scaling theory: all models that scale up gas exchange from leaf-level models require assumptions about photosynthetic resource allocation among leaves and over time. A common assumption, and which underlies the big-leaf scaling method, is that photosynthetic capacity is allocated in proportion to local irradiance (photosynthetic photon flux density) (Sellers *et al*. 1992; Amthor 1994). This assumption is popular for two reasons: firstly, it is widely perceived to be identical to optimal N allocation and, therefore, consistent with natural selection (Field 1983a; Hirose & Werger 1987; Sands 1995), and secondly, if leaf absorptance is invariant among leaves and if the time-averaged and instantaneous profiles of irradiance are equivalent, it renders models of leaf photosynthesis scale-invariant, and therefore applicable at crown scales (Farquhar 1989). Most data indeed show that photosynthetic capacity is positively correlated with local irradiance within crowns. However, the correlation is not linear; instead, it seems to saturate at high light, such that the photosynthetic capacity per unit of incident irradiance declines up through the crown (e.g. Fig. 1) (Evans 1993; Hirose & Werger 1994; Hollinger 1996; de Pury & Farquhar 1997; Makino *et al*. 1997; Bond *et al*. 1999; Friend 2001; Frak *et al*. 2002; Kull 2002; Lloyd *et al*. 2010) (but see Gonzales-Real & Baille 2000). Thus, photosynthetic nitrogen appears to be distributed suboptimally in relation to irradiance.

Many hypotheses have been offered to explain this apparent discrepancy. Some are economic: for example, that costs of reallocating N from old, shaded leaves to younger upper-crown leaves override the benefits (Field 1983a), or that the 'goal' of allocation is not simply crown net carbon gain, but perhaps something else that favours a different distribution of N (Hollinger 1996; Makino *et al*. 1997; Ackerly 1999; Schieving & Poorter 1999; Kull 2002). Other explanations are physiological or structural: for example, that the mechanisms underlying allocation (or reallocation) of N cannot achieve optima across the very wide range of irradiances encountered in deep canopies (Evans 1993; Pons & Pearcy 1994; Terashima & Hikosaka 1995b), perhaps because of leaf mass per unit area (LMA) being limited by structural constraints (Dewar *et al*. 2012) or by photosynthetic capacity being limited by physiological constraints (Lloyd *et al*. 2010).

Another class of explanations has not been thoroughly explored, in our view: namely, that optimization does not, in fact, predict a direct proportionality between capacity and irradiance. Published tests of optimization theory in real plant crowns typically calculate optimal distributions using simplified models, and those models may exclude features that affect the economics of nitrogen use in photosynthesis. One such feature that is of central interest in the present study is the supply of carbon dioxide to the mesophyll.

Corresponding author: T. N. Buckley. e-mail: tom.buckley@sonoma.edu

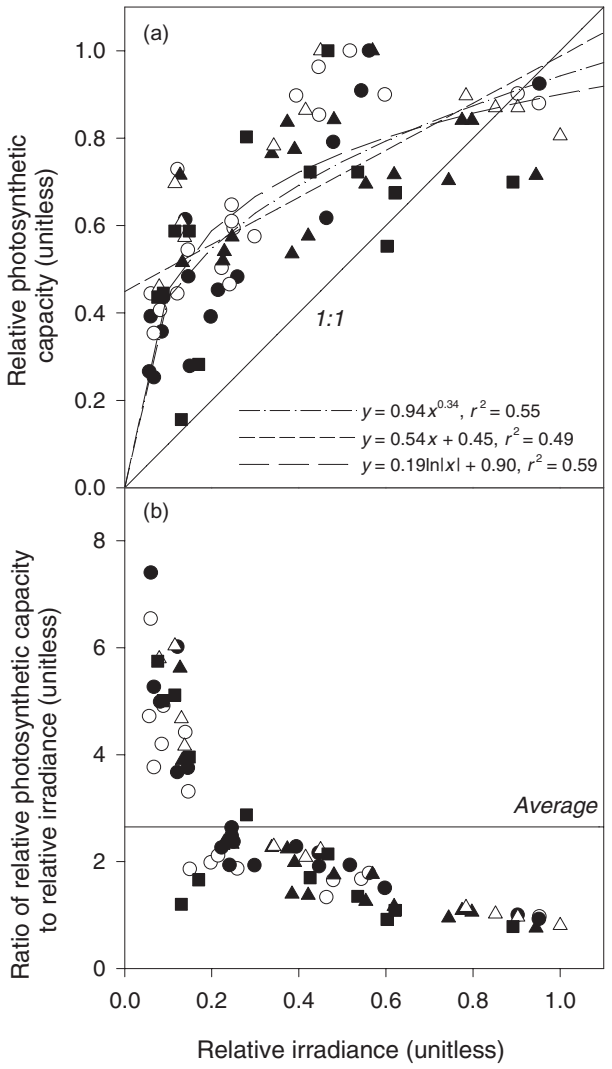

Figure 1. Sample observed relationships between photosynthetic capacity and irradiance from published data, showing the saturating nature of capacity versus irradiance. Values were normalized within each dataset and are shown as relative values. Symbols in (a) represent different species: closed circles, *Tsuga heterophylla*; open circles, *Pseudotsuga menziesii*; closed triangles, *Pinus ponderosa*; open triangles, *Juglans nigra* × *regia*; closed squares, *Nothofagus fusca*. In (a), three best-fit relationships are shown for all data combined (details given in the legend); the solid line is a 1:1 line. In (b), data from (a) are shown with photosynthetic capacity expressed as a ratio with relative irradiance; the horizontal line is the mean of all data shown. [Sources: *Nothofagus*: Hollinger (1996); *Tsuga*, *Pseudotsuga*, *Pinus*: Bond *et al.* (1999); *Juglans*: Frak *et al.* (2002)]. Capacity was given as maximum RuBP carboxylation rate for *Juglans* and as light-saturated net CO_2 assimilation rate for the other data.

Earlier authors have argued that the economics of N allocation cannot be fully understood without also considering the economics of stomatal transpiration (Field, Merino & Mooney 1983; Buckley, Miller & Farquhar 2002; Farquhar, Buckley & Miller 2002). Indeed, it is now well known that, just as the coordination of photosynthetic capacity with irradiance can vary systematically within crowns, so can the coordination of photosynthetic capacity with both stomatal and mesophyll conductance (Le Roux *et al.* 2001; Koch *et al.* 2004; Warren & Adams 2006; Burgess & Dawson 2007; Flexas *et al.* 2008). Peltoniemi, Duursma & Medlyn (2012) recently used a simple model to show that the ratio of optimal photosynthetic capacity to irradiance should be reduced in upper-crown leaves by hydraulic limitations to stomatal conductance. Similarly, Warren & Adams (2006) showed that photosynthetic nitrogen and water use efficiency are affected by physiological constraints on scaling of mesophyll conductance with photosynthetic capacity.

Other model features may also affect the calculation of optimal capacity profiles. de Pury & Farquhar (1997) showed that scale-invariance does not necessarily emerge from optimization when the key driving variable, local irradiance, varies in complex fashion over the day and with and within each canopy layer. Indeed, Bond *et al.* (1999) suggested that the issue could not be properly addressed without a highly detailed three-dimensional model of crown light penetration. Badeck (1995) and Kull & Kruijt (1998) showed that within-leaf gradients of light and photosynthetic capacity can be important for crown-scale nitrogen allocation. Other studies have shown that photosynthetic nitrogen partitioning among functional pools, including light capture, RuBP carboxylation and regeneration and electron transport, varies with growth irradiance (e.g. Terashima & Inoue 1984; Evans 1987; Terashima & Evans 1988; Evans, 1989) (for review, see Terashima & Hikosaka 1995a; Hikosaka & Terashima 1996).

Each of these factors may affect computed optimal N profiles, yet no analysis to date has brought them together to re-evaluate the question, how *should* photosynthetic capacity scale with incident irradiance in plant crowns? As suggested by Niinemets (2012) and Buckley *et al.* (2002), a resolution of the apparent discrepancy between measured and optimal distributions may require the incorporation of 'more realism' in the models used to compute optima.

The objective of this study was to assess the role of six model features in calculation of optimal profiles of photosynthetic capacity: (1) realistic three-dimensional and multimodal crown distributions of irradiance; (2) optimizing N allocation to light capture; (3) the co-occurrence of fixed transdermal (within-leaf) gradients in photosynthetic capacity and dynamic transdermal gradients in light; (4) optimal regulation of stomatal diffusion; (5) limitations on the ability of mesophyll conductance to track photosynthetic capacity in a linear and homogeneous fashion; and (6) an upper limit to instantaneous leaf transpiration rate, which reflects the need to maintain leaf water potential above the threshold causing runaway xylem cavitation. We used a numerical model to identify simultaneous optima for allocation of photosynthetic nitrogen among functional pools and among leaves, and for stomatal conductance over time and among leaves, in a sample of 500 leaves from an artificial crown of 8000 leaves in which the three-dimensional distribution of irradiance was modelled using a ray-tracing technique (Cescatti & Niinemets 2004) and leaf gas exchange was simulated using a biochemical and biophysical model (Farquhar, von Caemmerer & Berry 1980, von Caemmerer & Farquhar

1981; Buckley & Farquhar 2004) that explicitly accounts for transdermal gradients of irradiance and photosynthetic capacity.

THE MODEL

Our simulations used a process-based model of leaf photosynthesis, applied to many leaves in the same individual plant crown. In each leaf, the model was constrained by four parameters that depend on nitrogen investment or transpiration rate: V_{m25}, J_{m25}, α and $g_{sw}(t)$, which are, respectively, maximum RuBP carboxylation velocity at 25 °C, maximum potential electron transport rate at 25 °C, leaf absorptance to photosynthetic irradiance and the diurnal time course of stomatal conductance to water vapour. Those four parameters were adjusted to satisfy mathematical criteria for optimality. The model and optimization procedures are briefly summarized below, and additional details are given in the Appendix.

Gas exchange model

We used the photosynthesis and photorespiration model of Farquhar *et al*. (1980) to calculate mesophyll CO_2 demand as a function of chloroplastic CO_2 concentration (c_c), and expressions for CO_2 and H_2O diffusion given by von Caemmerer & Farquhar (1981) to calculate CO_2 supply to the chloroplast and transpiration rate. Our implementation of this widely used model was distinct from most previous implementations in two respects. Firstly, we specified mesophyll conductance to CO_2, g_m, by one of two alternative assumptions (that g_m is proportional to V_{m25}, or that g_m is invariant through the crown) and we assessed these alternatives in different simulations. Secondly, to account for the nitrogen cost of light capture in leaves of differing orientation and irradiance, we used a new model for whole leaf potential electron transport rate, J, that accounts for variable illumination at either leaf surface and variable transdermal gradients of photosynthetic capacity within leaves (Buckley & Farquhar 2004). In that model, the transdermal capacity profile is a weighted average of exponential profiles from either leaf surface, the weights being w_u and $w_l = 1 - w_u$ for the upper and lower surfaces, respectively. This model is described in the Appendix.

The simulated canopy comprised a uniform layer of random leaves with spherical leaf angle distribution.

Direct and diffuse irradiance at each leaf were simulated using a ray-tracing approach (Cescatti & Niinemets 2004), described in the Appendix. We used these irradiances to compute two values for all gas exchange variables for each leaf at each point in time: one for sunny conditions and one for cloudy conditions. Under perfectly cloudy conditions, light is entirely diffuse and thus unimodal, whereas under sunny conditions, most light is direct, creating a bi- or multimodal light environment. A weighted average of the sunny and cloudy values for leaf net CO_2 assimilation rate was then computed using the instantaneous probability of sunny conditions (p_{sun}) and its complement as the weights. This simulates an environment in which the radiation regime switches back and forth between sunny and cloudy conditions during a single day. p_{sun} was arbitrarily varied in different simulations to represent sunny, moderate or cloudy environments (p_{sun} = 0.9, 0.5 or 0.1, respectively).

Optimization method

Optimization of nitrogen and water are governed by the marginal water and nitrogen costs of fixed carbon: $\partial E/\partial A$ and $\partial N/\partial A_d$ (where A_d is the average of A over the day). When nitrogen and water are optimally allocated, these marginal costs are invariant: $\partial N/\partial A_d$ is invariant among leaves and among photosynthetic N pools, and $\partial E/\partial A$ is invariant among leaves and over time (Cowan & Farquhar 1977; Field 1983b; Farquhar 1989; Buckley *et al*. 2002). The four physiological parameters that affect $\partial E/\partial A$ and $\partial N/\partial A_d$ and are determined by resource investment (g_{sw}, V_{m25}, J_{m25} and α) were adjusted to achieve arbitrarily chosen target values for the marginal costs: the target value for $\partial N/\partial A_d$ was defined as ν, and the target value for $\partial E/\partial A$ was defined as λ. The numerical values of λ and ν were arbitrarily chosen (1100 mol H_2O $mol^{-1}CO_2$ and 0.22 mol N $dmol^{-1}$ CO_2, respectively) to give reasonable values for leaf gas exchange variables. This optimization was achieved in a series of nested loops. An 'outer' loop identified the leaf photosynthetic nitrogen content (N_p) for which $\partial N/\partial A_d = \nu$. For each candidate value of N_p in the outer loop, a second loop optimized the partitioning of that N_p among three pools, each serving a different photosynthetic function: N_v, RuBP carboxylation; N_j, RuBP regeneration and electron transport; and N_c, light capture. For each candidate vector of pool-wise N allocation fractions, a third loop optimized g_{sw} for each time point over the day. Detailed costing (relationships between resource investment and resource-dependent photosynthetic parameters) and numerical methods used in each loop are given in the Appendix.

Simulations

We performed a range of simulations to assess the effect of the seven model features outlined in the Introduction on inferred optimal crown distributions of photosynthetic capacity in relation to irradiance. In most cases, we compared a 'default' simulation with another in which some feature was omitted from, or altered relative to the model. The default simulation used the model as described above: that is, photosynthetic N was optimized for each functional pool, stomatal conductance was optimized at each time point and for each leaf, mesophyll conductance was assumed proportional to carboxylation capacity, potential electron transport rate (J) was calculated using the transdermally explicit model of Buckley & Farquhar (2004) with w_u (the weighting of the transdermal capacity profile to the upper surface) set equal to the fraction of daily irradiance received at the upper surface for each leaf, and the sunshine probability parameter p_{sun} was set at 0.5. The other simulations differed from the default simulation as follows:

1 *Cloudy or sunny conditions*: To assess the role of realistic three-dimensional and multi-modal crown distributions of

irradiance, we compared simulations under three scenarios for the degree of cloudiness of the above-crown light environment: $p_{sun} = 0.1$ (cloudy), 0.5 (moderate) or 0.9 (sunny).

2 *Variable N investment in leaf absorptance (α)*: To assess the effects of optimizing N investment in light capture (N_c), we compared default simulations with another in which N_c (and hence leaf absorptance) was not optimized, but instead was identical for each leaf [such that α was uniformly equal to its assimilation-weighted crown average from the default simulation (0.826)].

3 *Explicit transdermal gradients in capacity and light*: To assess the relevance of transdermal gradients in photosynthetic capacity and light (gradients among paradermal layers), we compared the default simulation with two others. In one, the bias of the transdermal capacity profile (w_u) was identical for all leaves and equal to its assimilation-weighted crown average from the default simulation (0.745); this accounts for transdermal light gradients but assumes transdermal capacity profiles cannot adapt to those gradients within each leaf independently. The other simulation used the standard model for J (a non-rectangular hyperbola), using the same curvature factor (θ_j, Eqn A7, Table 1) as in the default simulation; this ignores transdermal gradients entirely, which is equivalent to assuming transdermal profiles of capacity instantaneously adjust to match those of irradiance as the light regime shifts over the day (Buckley & Farquhar 2004).

4 *Variation in chloroplastic CO_2 (c_c)*: We assessed the role of optimal stomatal regulation by comparing the default simulation with another in which chloroplastic CO_2 concentration (c_c) was identical for each leaf and equal to its assimilation-weighted crown average from the default simulation (225 μmol mol^{-1}), instead of being set by optimization of stomatal conductance (g_s). Because optimization of g_s leads to smaller *computed* values of $\partial A/\partial N$ at any given level of photosynthetic N investment, this simulation used a smaller value of v (0.152 mol N dmol^{-1} CO_2) to yield the same whole-crown photosynthetic N content as the default simulation.

5 *Constraints on mesophyll conductance (g_m)*: We assessed the role of constraints on mesophyll conductance by comparing the default simulation with another in which g_m was identical among leaves and equal to its assimilation-weighted crown average from the default simulation (0.34 mol m^{-2} s^{-1}), instead of being directly proportional to carboxylation capacity in each leaf as in the default simulation. Note that invariant g_m is intended as a limiting scenario and should not be viewed as a representation of empirically observed patterns of g_m.

6 *Constraints on transpiration rate (E)*: We assessed the role of constraints on hydraulic conductance and transpiration rate by comparing the default simulation with another in which transpiration rate for each leaf (E) was limited to a value, E_{max}, to represent limitations imposed by the need to prevent runaway xylem cavitation. When optimized g_s caused E to exceed E_{max} for a leaf, its g_s was reduced so that $E = E_{max}$. E_{max} was arbitrarily set at 0.002 mol m^{-2} s^{-1}, which corresponds roughly to $g_{s,ref} = 0.17$ mol m^{-2} s^{-1} in terms of the model of Oren *et al.* (1999), in which $g_s = g_{s,ref} - m \ln(D/\text{kPa})$, where D is evaporative demand in kPa and $m = 0.6 \cdot g_{s,ref}$ (Oren *et al.* 1999, 2001; Ewers *et al.* 2001). This is in a range typical for many tree species (Oren *et al.* 1999).

The purpose of these simulations is to investigate the effect of specific model features on optimized profiles of crown photosynthetic nitrogen. They should each be interpreted as a theoretical device to that end, or 'thought experiments' in which the model is used to probe relationships among crown properties in a way that would not be possible using experiments on real crowns in nature. As such, these simulations will, by design and by necessity, include features that are not empirically realistic.

RESULTS

Optimal crown photosynthetic resource distributions (default simulation)

Field observations of the ratio of V_{m25} to I_d are that it decreases systematically up the crown. Figure 1 illustrates this trend with published data from several species. Here, we examine the results of simulations (1)–(6) and seek indications of a similar decrease in our model. The fully optimized model predicts positive relationships between integrated daily irradiance (I_d) and carboxylation capacity (V_{m25}) that have positive curvature (Fig. 2), such that the ratio of V_{m25} to I_d *increases* systematically up through the crown (Fig. 3); that is, opposite to observations. Electron transport capacity (J_{m25}) and V_{m25} are linearly and homogeneously related (Fig. 4), but the proportion of photosynthetic N allocated to light capture declines as I_d increases (Fig. 5). Intercellular and chloroplastic CO_2 concentrations (c_i and c_c; Fig. 6a) are approximately invariant among leaves, except for a steep decrease in relation to I_d in a few leaves at very low I_d. The decrease occurs among leaves with exceptionally low carbon gain, suggesting these leaves would probably not be produced in real canopies (cf. vertical lines in Fig. 3, indicating values of I_d above which 90 or 95% of crown carbon gain occurred).

Water, nitrogen and light use efficiencies (WUE, PNUE and LUE, respectively) calculated from daily averages of leaf net carbon gain, transpiration rate and irradiance behaved quite differently from one another: WUE was nearly invariant among leaves, whereas LUE and PNUE both increased with I_d (Fig. 7a).

Effect of complex multi-modal light environment

Under sunny conditions ($p_{sun} = 0.9$), most relationships predicted by the model became more scattered than under moderate conditions ($p_{sun} = 0.5$), whereas relationships in cloudy conditions ($p_{sun} = 0.1$) were less scattered (Figs 2, 3 & 7). The ratio V_{m25}/I_d increased with I_d at all values of p_{sun}. LUE became highly variable under sunny conditions, whereas WUE and PNUE were less variable (Fig. 7). (Note that the scatter introduced by sunflecks in these simulations could be mistaken for the random variation typically seen in empirical data, so we wish to emphasize that these are simulations and not actual data.)

Table 1. Parameters and variables in this paper. Area-based units are per leaf area, except those marked with an asterisk (*), which are per ground area. 'Irradiance' means photosynthetic photon flux density

Description	Symbol	Units	Value
Leaf net CO_2 assimilation rate	A	μmol m^{-2} s^{-1}	–
Leaf absorptance to photosynthetic radiation	α	–	–
Crown daily average of net CO_2 assimilation	A_d	mol m^{-2} d^{-1}*	–
Demand expression for net CO_2 assimilation rate	A_D	μmol m^{-2} s^{-1}	–
Demand expression (e^- transport limited)	A_{Dj}	μmol m^{-2} s^{-1}	–
Demand expression (carboxylation limited)	A_{Dv}	μmol m^{-2} s^{-1}	–
Ratio of max photosynthetic rate (P_{max}) to [cyt *f*]	a_f	mol CO_2 s^{-1} mol^{-1} cyt *f*	19.9
Ratio of P_{max} to [PSII]	a_p	mol CO_2 s^{-1} mol^{-1} PSII	18.2
Ratio of [PSI] to [Chl]	a_s	mol PSII mol^{-1} Chl	$1.74{\cdot}10^{-3}$
Supply expression for net CO_2 assimilation rate	A_s	μmol m^{-2} s^{-1}	–
Solar elevation angle	β	degrees	–
Leaf chlorophyll content	[Chl]	mmol m^{-2}	–
Intercellular CO_2 mole fraction	c_i	μmol mol^{-1}	–
Chloroplastic CO_2 mole fraction	c_c	μmol mol^{-1}	–
Carboxylation capacity per N	χ_v	μmol CO_2 s^{-1} mmol^{-1} N	4.49
Electron transport capacity per N	χ_j	μmol e^- s^{-1} mmol^{-1} N	9.48
Chlorophyll per electron transport N (N_j)	χ_{cj}	mmol Chl mmol^{-1} N	$4.64{\cdot}10^{-4}$
Chlorophyll per light capture N (N_c)	χ_c	mmol Chl mmol^{-1} N	$3.384{\cdot}10^{-2}$
Cytochrome *f* per unit group II N	χ_{II}	mol cyt *f* mol^{-1} N	1/9530
PSII per unit group III N	χ_{III}	mol cyt *f* mol^{-1} N	1/5000
PSI per unit group IV N	χ_{IV}	mol cyt *f* mol^{-1} N	1/6040
Chl per unit group III N	χ_{cIII}	mol Chl mol^{-1} N	1/83.3
Chl per unit group IV N	χ_{cIV}	mol Chl mol^{-1} N	1/32.8
Chl per unit group V N	χ_{cV}	mol Chl mol^{-1} N	1/26.0
Solar declination	δ	degrees	–
Time step	δt	hours	–
Marginal carbon product of water use	$\partial E/\partial A$	mol mol^{-1}	–
Marginal carbon product of nitrogen use	$\partial N/\partial A_d$	mol [mol d^{-1}]$^{-1}$	–
Leaf transpiration rate	E	mol m^{-2} s^{-1}	–
Fraction of absorbed photons not used in photosynthesis	F	e^-/photon	0.23
Light-capture fraction of photosynthetic N	f_c	–	–
Diffuse fraction of daily irradiance	f_d	–	–
Electron transport fraction of photosynthetic N	f_j	–	–
Carboxylation fraction of photosynthetic N	f_v	–	–
Shortwave radiation	Φ	J m^{-2} s^{-1}	–
Photorespiratory CO_2 compensation point	Γ_* (Γ_{*25})	μmol mol^{-1}	–, 36.9
Boundary layer conductance to CO_2 (H_2O)	g_{bc} (g_{bw})	mol m^{-2} s^{-1}	–
Boundary layer conductance to heat	g_{bh}	mol m^{-2} s^{-1}	–
Mesophyll conductance to CO_2	g_m	mol m^{-2} s^{-1}	–
Stomatal conductance to CO_2 (H_2O)	g_{sc} (g_{sw})	mol m^{-2} s^{-1}	–
Total conductance to CO_2 (H_2O)	g_{tc} (g_{tw})	mol m^{-2} s^{-1}	–
Beam irradiance at upper (lower) leaf surface	I_{bu} (I_{bl})	μmol m^{-2} s^{-1}	–
Integrated daily irradiance	I_d	mol m^{-2} d^{-1} *	–
Diffuse irradiance at upper (lower) leaf surface	I_{du} (I_{dl})	μmol m^{-2} s^{-1}	–
Diffuse (beam) irradiance above crown	I_{od} (I_{ob})	μmol m^{-2} s^{-1}	–
Irradiance at upper (lower) leaf surface	I_u (I_l)	μmol m^{-2} s^{-1}	–
Global irradiance (above atmosphere)	I_{og} (I_o)	μmol m^{-2} s^{-1}	–
Leaf potential e^- transport rate	J	μmol m^{-2} s^{-1}	–
Day of year	J_{day}	–	0
Light-limited maximum potential e^- transport rate	J_i	μmol m^{-2} s^{-1}	–
Leaf maximum potential e^- transport rate (at 25 °C)	J_m (J_{m25})	μmol m^{-2} s^{-1}	–
Excess J_i in light-saturated transdermal layers	J_s	μmol m^{-2} s^{-1}	–
Michaelis constant for RuBP carboxylation (at 25 °C)	K_c (K_{c25})	μmol mol^{-1}	–, 404
Michaelis constant for RuBP oxygenation (at 25 °C)	K_o (K_{o25})	kPa	–, 24.8
Setpoint for $\partial E/\partial A$	λ	mol mol^{-1}	1100
Crown daily light use efficiency	LUE	mol mol^{-1}	–
Setpoint for $\partial N/\partial A_d$	ν	mol d mol^{-1}	0.22
Light capture nitrogen	N_c	mmol N m^{-2}	–
Electron transport nitrogen	N_j	mmol N m^{-2}	–
Photosynthetic N	N_p	mmol N m^{-2}	–
Rubisco nitrogen	N_v	mmol N m^{-2}	–

Table 1. *Continued*

Description	Symbol	Units	Value
Group I N (Rubisco)	N_I	mmol N m^{-2}	–
Group II N (electron transport, Calvin cycle)	N_{II}	mmol N m^{-2}	–
Group III N (PSII)	N_{III}	mmol N m^{-2}	–
Group IV N (PSI, LHCI)	N_{IV}	mmol N m^{-2}	–
Group V N (LHCII)	N_V	mmol N m^{-2}	–
Oxygen concentration	O	kPa	21
Crown daily photosynthetic N use efficiency	PNUE	mol d^{-1} mmol^{-1}	–
Instantaneous sunshine probability	p_{sun}	–	0.5
Curvature factor for photosynthesis	θ_A	–	0.99
Curvature factor for electron transport	θ_j	–	0.86
Non-photorespiratory CO_2 release in the light (at 25 °C)	R_d (R_{d25})	μmol m^{-2} s^{-1}	–, $0.0089V_{m25}$
Time of day	t	h	–
Air temperature (in Kelvin)	T_a (T_{aK})	°C, K	–
Leaf temperature (in Kelvin)	T_l (T_{lK})	°C, K	–
Wind speed (at top of crown)	v (v_o)	m s^{-1}	–, 5
Leaf maximum carboxylation rate (at 25 °C)	V_m (V_{m25})	μmol m^{-2} s^{-1}	–
Downwind leaf width	w	m	0.12
Water vapour mole fraction of the air	w_a	mol mol^{-1}	1.0
Saturation water vapour mole fraction of the air	w_{sa}	mol mol^{-1}	–
Saturation water vapour mole fraction in leaf	w_{sl}	mol mol^{-1}	–
Bias of transdermal capacity profile to upper leaf surface	w_u	–	–
Crown daily water use efficiency	WUE	mol kmol^{-1}	–

Effect of optimizing nitrogen allocation to light capture

When leaf absorptance was held invariant among leaves in simulations at moderately sunny conditions ($p_{sun} = 0.5$), the relationship between V_{m25} and I_d became approximately linear and homogeneous, such that the ratio V_{m25}/I_d did not increase with I_d (Fig. 8).

Effect of explicit transdermal gradients in capacity and irradiance

The shape of the relationship between V_{m25} and I_d was indistinguishable between the default simulation and those in which the bias of the transdermal capacity profile (w_u) was identical among leaves, or in which transdermal gradients in capacity and irradiance were ignored altogether (not shown).

Effect of optimal stomatal regulation

The relationship between V_{m25} and I_d was broadly similar whether g_s was optimized (and g_m was set proportional to V_{m25}) or c_c was set as a constant, equal to the crown average from the optimized default scenario (Fig. 9). In the latter case – in which g_s and g_m were irrelevant to carbon gain – the relationship between V_{m25} and I_d exhibited slightly more scatter at any given I_d.

Effect of constraints on mesophyll conductance

When g_m was assumed invariant among leaves, the ratio V_{m25}/I_d decreased slightly with I_d across most of the range of I_d (Fig. 10), and c_c systematically declined with I_d, whereas c_i increased (Fig. 6b).

Effect of constraints on leaf transpiration rate

When instantaneous leaf transpiration rate was limited to an imposed maximum value, the relationship between V_{m25} and I_d took on clear negative curvature, such that the ratio V_{m25}/I_d declined with increasing I_d across most of the range of I_d (Fig. 10). Assimilation-weighted average c_i and c_c both declined with increasing I_d in this simulation (Fig. 6c).

DISCUSSION

The objective of this study was to ask a theoretical question rather than an empirical one: does the apparent discrepancy between observed and optimal crown profiles of photosynthetic capacity disappear when certain detailed features are included in the models used to infer optimal profiles? This followed the suggestion by Niinemets (2012) that the discrepancy could not be adequately understood without incorporation of greater realism in models. Our analysis took the form of a series of 'thought experiments': we performed a default simulation using a model that included many detailed features that were meant to impart realism, and then these features were individually modified or excluded in subsequent simulations. The purpose of these thought experiments was to determine how these features affect calculated optimal crown capacity profiles. The main dependent variable of interest in these comparisons was the ratio of carboxylation capacity to integrated daily irradiance (V_{m25}/I_d). This is because observations typically show the ratio V_{m25}/I_d decreasing up through the crown (e.g. Fig. 1), whereas most previous theoretical studies have concluded that this ratio should be invariant with I_d – that is, in the optimum, V_{m25} should be linearly and homogeneously related to I_d. Therefore, we

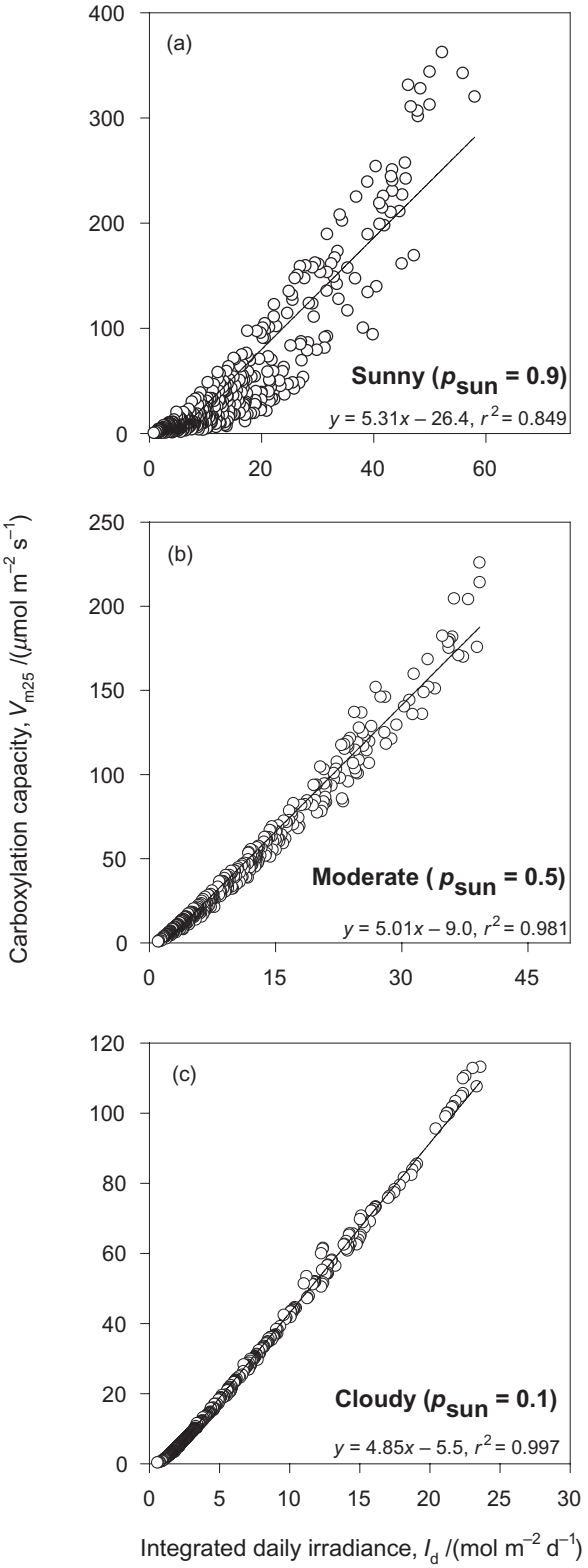

Figure 2. Optimal relationships between daily irradiance, I_d, and carboxylation capacity at 25 °C, V_{m25}, under different sunshine probabilities (p_{sun}): (a) $p_{sun} = 0.9$ (sunny); (b) $p_{sun} = 0.5$ (moderate, default simulation); and (c) $p_{sun} = 0.1$ (cloudy). Each point is a different leaf in the same crown. Best-fit lines and their equations and coefficients of determination are shown.

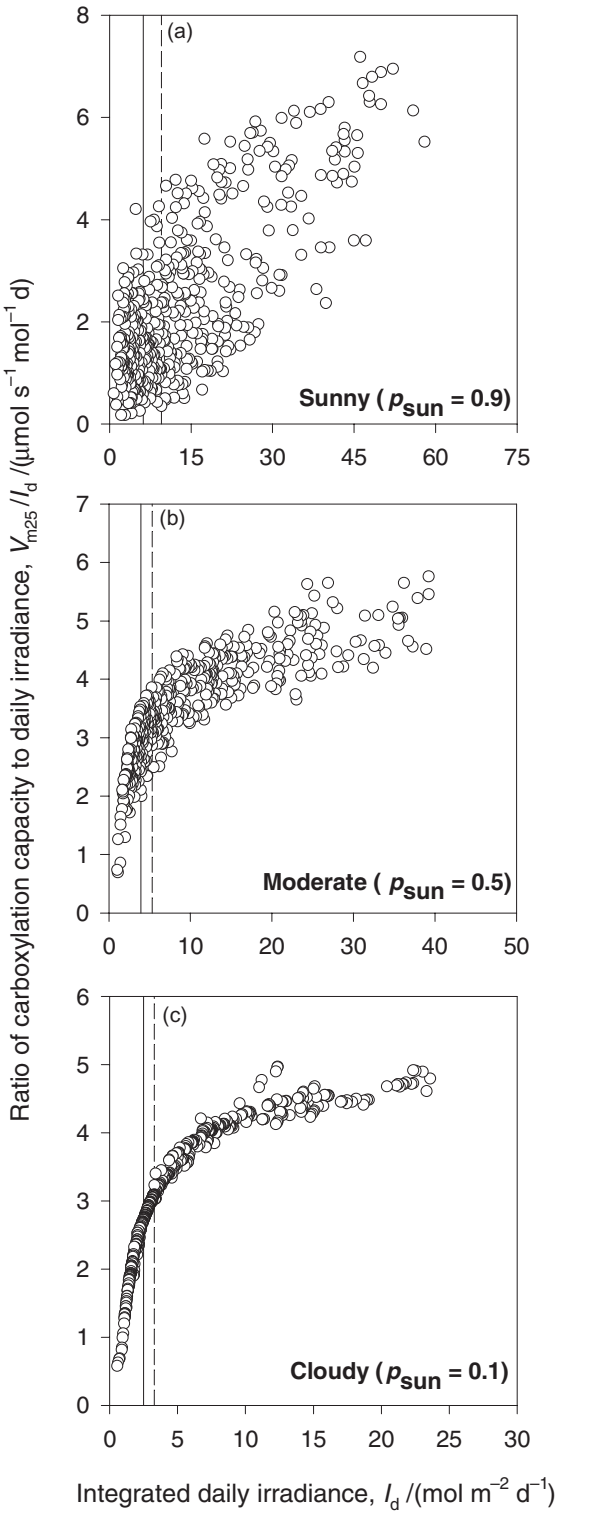

Figure 3. Ratio of carboxylation capacity at 25 °C, V_{m25}, to daily incident irradiance, I_d, shown in relation to I_d, under different sunshine probabilities (p_{sun}): (a) $p_{sun} = 0.9$ (sunny); (b) $p_{sun} = 0.5$ (moderate, default simulation); and (c) $p_{sun} = 0.1$ (cloudy). The vertical lines indicate leaves whose daily net carbon gain (A_d) is such that whole-crown daily net carbon gain would only decline by 5% (solid lines) or 10% (dashed lines) if leaves with equal or lower A_d were excluded.

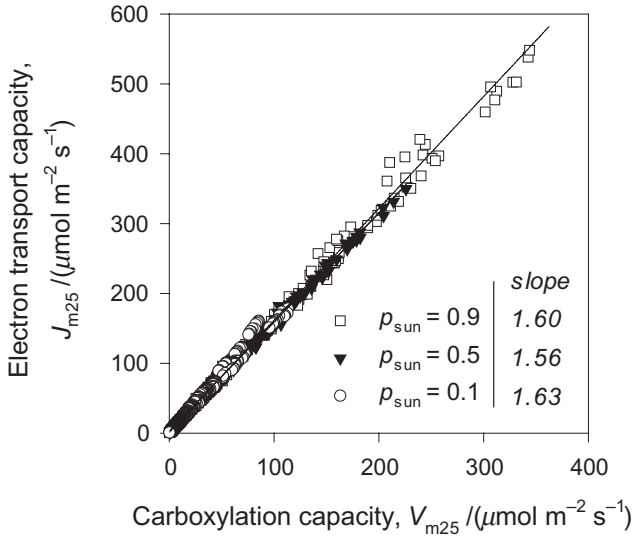

Figure 4. Relationship between carboxylation capacity (V_{m25}) and electron transport capacity (J_{m25}) among leaves in crowns that were optimized under different sunshine probabilities (p_{sun}): open circles, $p_{sun} = 0.1$; closed triangles, $p_{sun} = 0.5$ (default simulation); open squares, $p_{sun} = 0.9$. Slopes of lines fitted to relationships for each p_{sun} value are given in the legend.

asked whether various model details would alter this conclusion, predicting instead that V_{m25}/I_d should *decrease* with increasing I_d in the optimum, as is observed in the field.

Allowing N investment in light capture to vary optimally makes the discrepancy worse

In our default simulation, the ratio V_{m25}/I_d increased with I_d. This is in part because our model allowed leaf absorptance, α,

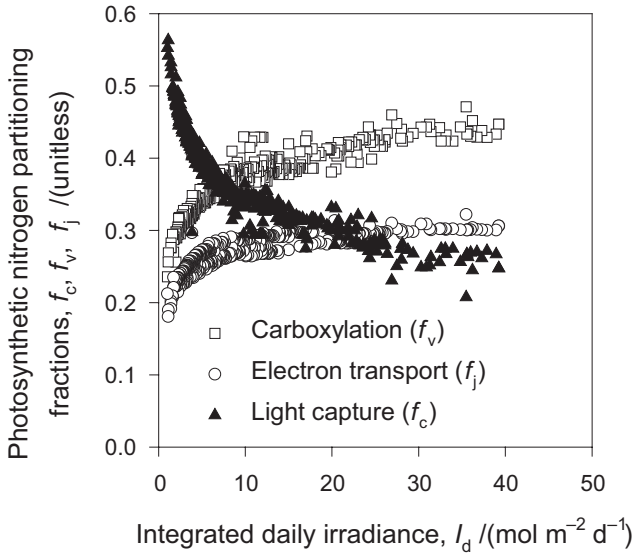

Figure 5. Photosynthetic nitrogen partitioning fractions (f_c, light capture; f_v, carboxylation; f_j, electron transport) in the default simulation. Each point is a different leaf in the same crown.

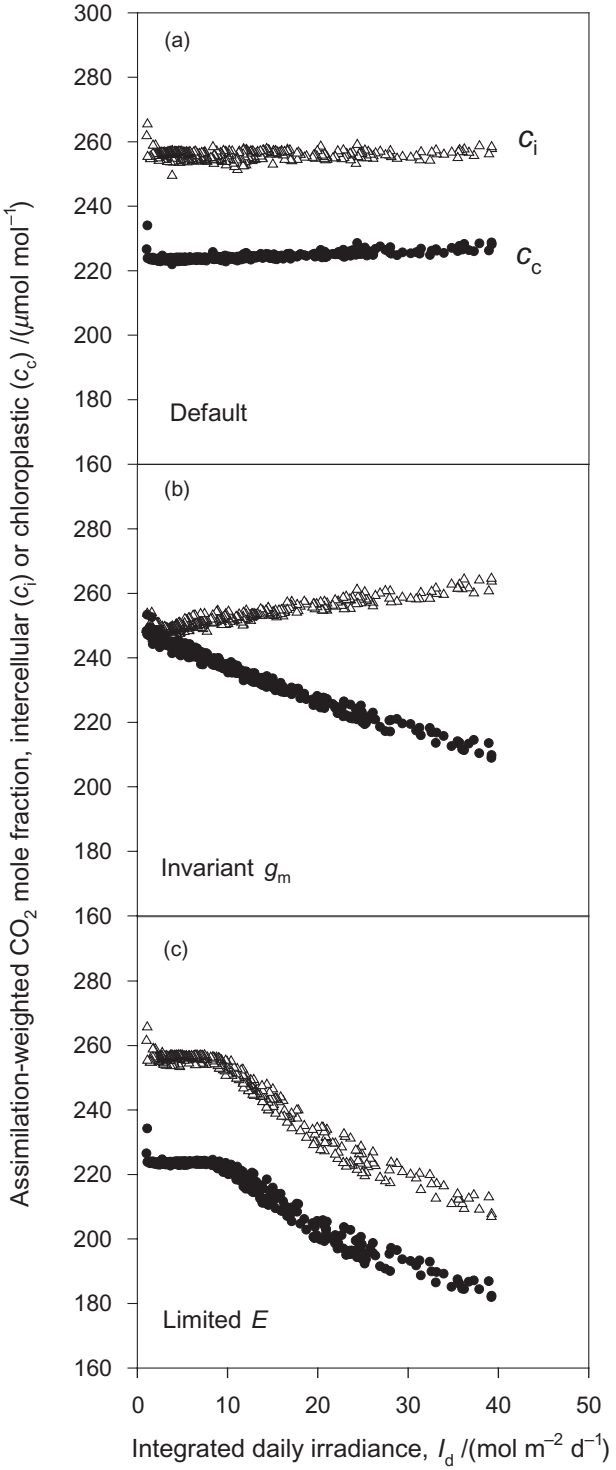

Figure 6. Relationships between assimilation weighted CO_2 concentration [intercellular, c_i (open triangles); chloroplastic, c_c (closed circles)] and integrated daily irradiance (I_d) for crowns optimized with different assumptions about the regulation of CO_2 supply to the mesophyll: (a) stomatal conductance (g_s) optimized and mesophyll conductance (g_m) proportional to carboxylation capacity (default simulation; no arbitrary constraints on CO_2 supply); (b) as in (a), but with g_m invariant among leaves; (c) as in (a), but with g_s indirectly constrained by an upper limit (E_{max}) on transpiration rate (E).

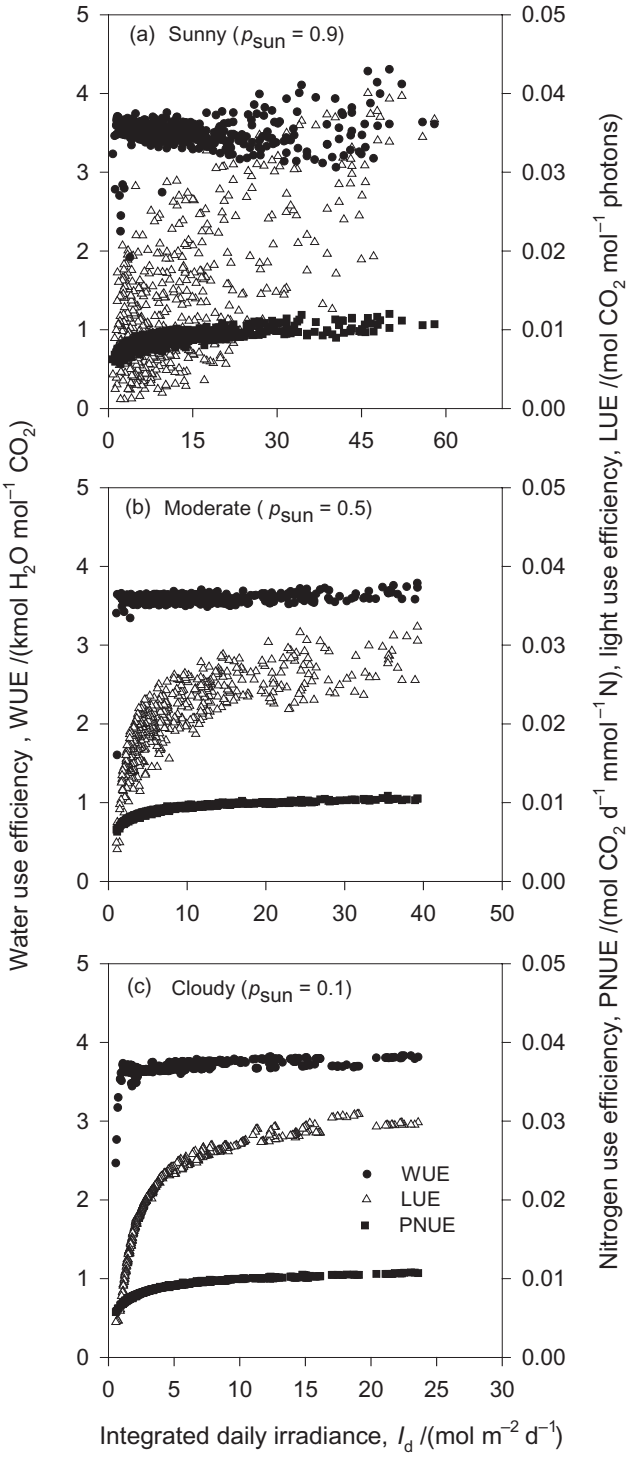

Figure 7. Predicted crown profiles in photosynthetic resource efficiency (ratios of daily net carbon gain to resource use): water use efficiency, WUE (left axis, closed circles), photosynthetic nitrogen use efficiency, PNUE (right axis, closed squares) and light use efficiency, LUE (right axis, open triangles) for a crown optimized under (a) sunny conditions (p_{sun} = 0.9) (default simulation), (b), moderate conditions (p_{sun} = 0.5) or (c) cloudy conditions (p_{sun} = 0.1).

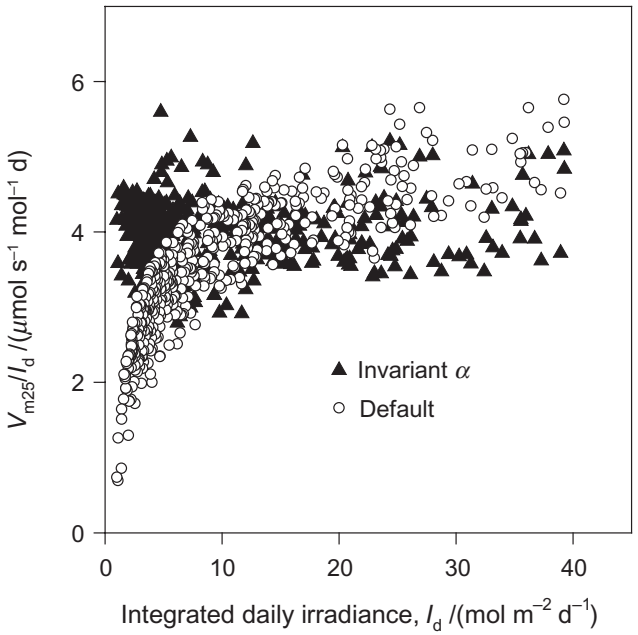

Figure 8. Relationships between integrated daily irradiance (I_d) and the ratio of carboxylation capacity, $V_{m25,}$ to I_d, for simulations in which leaf absorptance was held invariant among leaves (closed triangles) or was allowed to vary among leaves such that N investment in light capture was optimized (open circles, default simulation). These simulations were performed under moderately sunny conditions (p_{sun} = 0.5).

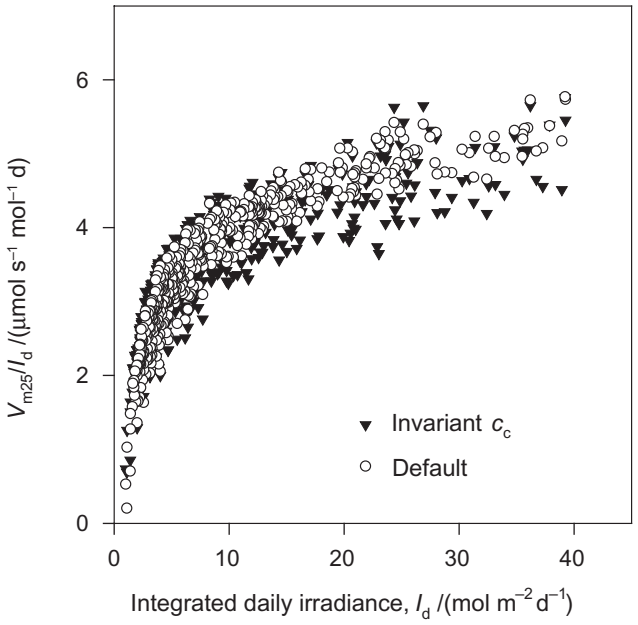

Figure 9. Relationships between integrated daily irradiance (I_d) and the ratio of carboxylation capacity, $V_{m25,}$ to I_d, when stomatal conductance was optimized (default simulation, open circles) or chloroplastic CO_2 concentration, c_c, was invariant among leaves and equal to the assimilation-weighted average from the default simulation.

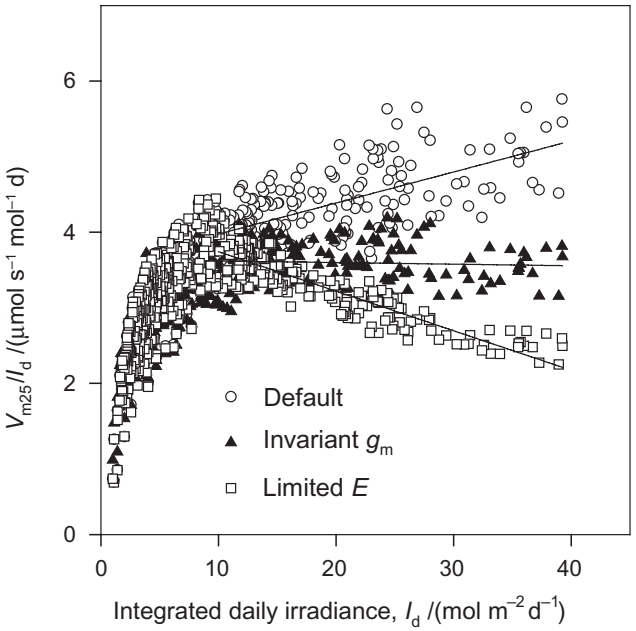

Figure 10. Relationships between integrated daily irradiance (I_d) and the ratio of carboxylation capacity, V_{m25}, to I_d, for two alternative simulations that included *ad hoc* constraints on mesophyll CO_2 supply (closed triangles and open squares) not present in the default simulation (open circles). Closed triangles ('invariant g_m'), mesophyll conductance, g_m, invariant among leaves. Open squares ('limited E'), stomatal conductance indirectly limited by an upper bound (E_{max}) on transpiration rate (E). Best-fit lines for values above $I_d = 10$ mol m^{-2} d^{-1} are shown for each case.

to vary among leaves as needed to optimize N investment in light capture. The result of this optimization was that α increased with I_d, which caused *absorbed* irradiance to increase non-linearly and with positive curvature in relation to incident irradiance. Because absorbed irradiance, not incident irradiance *per se*, determines the return on N investment in carboxylation and electron transport capacities (V_{m25} and J_{m25}), these capacities therefore also increased non-linearly with I_d, and therefore the ratio V_{m25}/I_d also increased with I_d (e.g. Fig. 3). Previous authors have pointed out that leaf absorptance should be greater in high light than in low light (e.g. Evans 1989; Hikosaka & Terashima 1995), yet few analyses of optimal N allocation in crowns have allowed absorptance to vary. Our simulations suggest, in any event, that including this feature does not resolve the discrepancy between actual and optimal capacity profiles, but instead it makes it worse.

Accounting for transdermal gradients in light and capacity has little impact

We found that explicitly accounting for transdermal gradients of irradiance and photosynthetic capacity had no qualitative effect on predicted optimal profiles of photosynthetic capacity. This contrasted with the conclusions of Badeck (1995), who also used a transdermally explicit model. However, that model made two assumptions that differed from our own: it assumed that photosynthetic capacity per unit chlorophyll was identical in all transdermal layers, and that V_{m25} and J_{m25} were directly proportional to leaf Chl content among leaves. Those assumptions ensured that partitioning of photosynthetic N among light capture, carboxylation and electron transport could not vary with irradiance. As a result, the return from N investment in light capture declined as I_d increased in that model. This, in turn, required reduced investment in photosynthetic capacity relative to irradiance at high light (in order to keep the marginal N cost of carbon, $\partial N/\partial A_d$, invariant among leaves as required for optimization), so predictions from that model are more in line with observations. By contrast, our simulations used the model of Buckley & Farquhar (2004), which assumes the transdermal profile of capacity is a weighted average of exponential profiles that decline from either leaf surface. We also allowed N partitioning to vary with irradiance by optimising N allocation to light capture, carboxylation and regeneration separately. This captures the tendency for photosynthetic partitioning to acclimate to local environmental conditions, both within and among leaves. In short, the contrast between our results and those of Badeck (1995) results from greater flexibility of photosynthetic partitioning in our model, so if partitioning is in fact somehow constrained in real crowns, that could help explain the discrepancy between observed and optimal capacity profiles.

Constraints on CO_2 supply to the mesophyll help resolve the discrepancy

Most previous analyses of optimal crown N allocation have either assumed a constant value for intercellular or chloroplastic CO_2 concentration (c_i or c_c, respectively), either implicitly or explicitly (Hirose & Werger 1987; Gutschick & Wiegel 1988; Evans 1993; Hikosaka & Terashima 1995; Sands 1995; Ackerly 1999; Bond *et al.* 1999), or have specified stomatal conductance (g_{sw}) using empirical models that assume g_{sw} is linearly proportional to photosynthetic rate (Field 1983a; Hollinger 1996; Haefner, Buckley & Mott 1997). Our results suggest that those assumptions are reasonable proxies for optimal stomatal behaviour because predictions from our model were qualitatively similar whether g_{sw} was optimized over time and among leaves, or if instead the general character of stomatal control was represented indirectly, by holding c_c constant. In particular, optimization of g_{sw} did not give rise to any systematic trends in c_i or c_c in relation to irradiance in the default simulation.

However, when the model incorporated features that caused CO_2 supply to the mesophyll to decline systematically in relation to increasing irradiance, the ratio V_{m25}/I_d also declined with increasing I_d across most of the range of I_d. This result held whether CO_2 supply was restricted by limitations on mesophyll or stomatal conductance, although the effect was far greater in the latter case (e.g. Fig. 10). The reason that lower photosynthetic capacity is optimal if c_c is lower is simply that the marginal carbon product of N, $\partial A_d/\partial N$, is positively related to c_c and negatively to photosynthetic N (Buckley *et al.* 2002); thus, to maintain invariance among leaves in $\partial A_d/\partial N$ as required for optimality, a decrease in c_c necessitates a decrease in photosynthetic N investment.

Hydraulic constraints in relation to height are well known and widely studied (Yoder *et al*. 1994; Hubbard, Bond & Ryan 1999; Ryan *et al*. 2000; Phillips *et al*. 2002; Delzon *et al*. 2004; Franks 2004; Ryan, Phillips & Bond 2006), so such constraints may help explain the apparent discrepancy between observed and optimal photosynthetic capacity – at least in tall trees, where height is likely to substantially limit hydraulic conductance. In this respect, our results echo those of Peltoniemi *et al*. (2012), who used a simple two-leaf model, in which stomatal conductance, was directly proportional to hydraulic conductance, to show that optimal photosynthetic N investment should be reduced in upper crown leaves experiencing hydraulic limitation. However, this explanation is unlikely to explain the discrepancy in very short canopies, such as crops like wheat (e.g. de Pury & Farquhar 1997).

Evidence also suggests that g_m can only track photosynthetic capacity up to a point, beyond which it saturates (Niinemets *et al*. 2005, 2006; Warren & Adams 2006), probably due to limits to leaf structural plasticity (Flexas *et al*. 2012). Because relationships between g_m and V_{m25} vary widely and cannot be generalized (Flexas *et al*. 2012), we used two limiting cases to bound the range of constraints on g_m – either g_m tracked V_{m25} perfectly, or it was held invariant among leaves. When the crown was optimized under invariant g_m, V_{m25}/I_d declined slightly across most of the range of irradiance. Thus, constraints on g_m can, in theory at least, contribute to reconciling observed and inferred optimal crown N profiles. However, that simulation also made an unrealistic prediction, namely that c_i *increases* up through the crown. This occurred because the g_m constraint reduced N investment in photosynthetic capacity at high irradiance (which is, of course, the very phenomenon that we set out to explain), but this, in turn, reduced total CO_2 demand, leading to the increase in c_i. Our results thus suggest that while g_m constraints may contribute to reconciling the discrepancy between optimal and observed capacity profiles, they must be combined with another factor that independently reduces c_i. As we found much stronger reductions in V_{m25}/I_d with increasing I_d when g_{sw} was constrained than when g_m was constrained, we conclude that hydraulic constraints on g_{sw} remain the strongest hypothesis to resolve the discrepancy.

Other explanations for the discrepancy between observed and optimal profiles

A variety of other arguments have been advanced to explain the apparent discrepancy between actual and optimal profiles of photosynthetic capacity. One class of arguments centres on the idea that crown net carbon gain is not the correct goal function to understand the adaptive significance of photosynthetic nitrogen allocation. For example, Ackerly (1999) suggested that leaf production and height growth are more important because of competition for light, and Schieving & Poorter (1999) showed how light competition between species could skew vertical profiles of photosynthetic capacity and reduce crown carbon gain. However, leaf construction and height growth represent investments of reduced carbon, not nitrogen (although leaves and wood do contain N) – leaves and wood devoid of N would suffice if their sole function were to cast shade on competitors, so these considerations do not bear on the optimal distribution of N *among leaves*. Kull (2002) suggested that the proper goal function is actually a compromise between maximizing carbon gain and maximizing PNUE, and that the costs of leaf construction must be included somehow; Hollinger (1996) made a similar suggestion. Yet, maximal PNUE must depend on the total supply of nitrogen, which leads to the question, how much carbon should be invested in roots? Thus, it seems again that crown carbon gain should nevertheless be maximized because carbon can be used to capture more N.

It has also been argued that lower-crown leaves that initially developed in higher-light conditions cannot fully remobilize photosynthetic nitrogen when they begin to become shaded (Hikosaka & Terashima 1995), or that the costs of remobilization skew optimal N distributions (Field *et al*. 1983). However, the cost of remobilizing N would not affect comparisons of $\partial N/\partial A_d$ among leaves, assuming that cost is directly proportional to N content: in that case, the remobilization cost would merely add a constant to $\partial N/\partial A_d$. Another possibility is that leaves store nitrogen in photosynthetically active pools such as Rubisco and electron transport chain components in order to hedge against future deficits, or as a reservoir for N acquired during vigorous early season growth when water and nitrogen are plentiful. The economic benefits of storage are difficult to express and have not been included in any analyses of crown N allocation, to our knowledge. However, delayed costs and benefits of water use have previously been addressed in the context of optimal stomatal control (Cowan 1977, 1986; Cowan & Farquhar 1977; Comins & Farquhar 1982), so the problem may be tractable. Our model also excludes temporal buffering of the light environment by non-steady-state photosynthesis (enabled by large potential pool sizes for photosynthetic intermediates) which can allow an intermediate photosynthetic rate to persist across sun- and shade-flecks (Pearcy 1990). Future analyses should consider these additional details.

Others have posited upper or lower limits on the properties of leaves within crowns in order to explain the tendency for profiles of capacity to be 'less steep' than those of irradiance. For example, Lloyd *et al*. (2010) suggested that photosynthetic capacity has an upper physiological limit, and Dewar *et al*. (2012) suggested that LMA has a lower limit. Both studies concluded that, for a given total capacity, crown photosynthesis is greatest if capacity profiles are less steep than irradiance profiles, once upper limits to capacity or lower limits to LMA are accounted for. However, both studies also assumed that the profile of capacity must follow an exponential curve. While such profiles may be empirically observed, there is no *a priori* reason to suppose they are optimal, in the sense that no possible redistribution of photosynthetic nitrogen among leaves would increase total carbon gain. The latter condition requires invariance of the marginal C product of N, $\partial A/\partial N$ (Field 1983a; Farquhar 1989), which, in turn, requires close proportionality between irradiance and capacity, unless, as we have shown here, another determinant of net photosynthesis, such as CO_2

supply, varies systematically with irradiance, or leaf absorptance is allowed to vary optimally among leaves. If a plant has acquired such a surfeit of available N that physiological bounds on capacity or LMA require the N to be allocated suboptimally, perhaps the carbon that was used to acquire that N could have been better invested to secure water or light – the other photosynthetic resources, which are partially substitutable for N (Schulze *et al*. 1998; Miller, Williams & Farquhar 2001; Miller 2002; Buckley & Roberts 2006). This does not imply that the data are wrong – that shallow exponential profiles, for example, those shown by Lloyd *et al*. (2010), do not occur, as they clearly do – but rather that the answer to the question 'what is optimal' depends entirely on what constraints are assumed in posing the question. In the present study, we sought to identify optima subject only to known biophysical constraints, so we chose not to impose upper or lower bounds on capacity. Observed limits on capacity may represent biophysical constraints, but this remains a hypothesis; they may, however, be emergent properties of the sort of resource interactions that we examined in this study. This question awaits experimental resolution.

CONCLUSIONS

We found that optimal crown distributions of photosynthetic nitrogen were affected by each of several features that had been excluded from most previous analyses. Some features caused the ratio of photosynthetic capacity to daily irradiance (V_{m25}/I_d) to increase up through the crown – at odds with observations – while others caused a decrease, in line with observations. When nitrogen investment in light capture was optimized along with investments in other photosynthetic pools, leaf absorptance was greater in the upper crown. Thus, *absorbed* irradiance and photosynthetic capacity increased faster than incident irradiance and V_{m25}/I_d was greater in the upper crown. Conversely, features that tended to reduce CO_2 supply to the mesophyll in the upper crown – including hydraulic constraints on stomatal conductance and limits on the ability of mesophyll conductance to track photosynthetic capacity at high light – caused V_{m25}/I_d to plateau or decline with increasing irradiance, as often reported for real crowns. We therefore conclude that, at present, constraints on mesophyll CO_2 supply that increase systematically up through the canopy seem best able to explain the apparent discrepancy between optimal and actual distributions of photosynthetic nitrogen. This highlights the importance of viewing plant and leaf function as an integrated whole, in which the adaptive significance of any one feature – photosynthetic N allocation in this instance – often cannot be understood independently from other features, as all traits may systematically covary as the plant adapts to environmental gradients or change.

ACKNOWLEDGMENTS

The authors acknowledge helpful comments from an anonymous reviewer on an earlier draft of this paper. T.N.B. thanks John Evans for informative discussions about nitrogen partitioning within leaves and acknowledges support from Australia's Cooperative Research Centre for Greenhouse Accounting in the early part of this work.

REFERENCES

Ackerly D.D. (1999) Self-shading, carbon gain and leaf dynamics: a test of alternative optimality models. *Oecologia* **119,** 300–310.

Amthor J.S. (1994) Scaling CO_2-photosynthesis relationships from the leaf to the canopy. *Photosynthesis Research* **39,** 321–350.

Badeck F.-W. (1995) Intra-leaf gradient of assimilation rate and optimal allocation of canopy nitrogen: a model on the implications of the use of homogeneous assimilation functions. *Australian Journal of Plant Physiology* **22,** 425–439.

Bernacchi C.J., Singsaas E.L., Pimentel C., Portis A.R.J. & Long S.P. (2001) Improved temperature response functions for models of Rubisco-limited photosynthesis. *Plant, Cell & Environment* **24,** 253–259.

Bond B.J., Farnsworth B.T., Coulombe R.A. & Winner W.E. (1999) Foliage physiology and biochemistry in response to light gradients in conifers with varying shade tolerance. *Oecologia* **120,** 183–192.

Buckley T.N. & Farquhar G.D. (2004) A new analytical model for whole-leaf potential electron transport rate. *Plant, Cell & Environment* **27,** 1487–1502.

Buckley T.N. & Roberts D.W. (2006) How should leaf area, sapwood area and stomatal conductance vary with tree height to maximise growth? *Tree Physiology* **26,** 145–157.

Buckley T.N., Miller J.M. & Farquhar G.D. (2002) The mathematics of linked optimisation for nitrogen and water use in a canopy. *Silva Fennica* **36,** 639–669.

Burgess S.S.O. & Dawson T.E. (2007) Predicting the limits to tree height using statistical regressions of leaf traits. *New Phytologist* **174,** 626–636.

von Caemmerer S. & Farquhar G.D. (1981) Some relationships between the biochemistry of photosynthesis and the gas exchange of leaves. *Planta* **153,** 376–387.

von Caemmerer S., Evans J.R., Hudson G.S. & Andrews T.J. (1994) The kinetics of ribulose-1,5-bisphosphate carboxylase/oxygenase in vivo inferred from measurements of photosynthesis in leaves of transgenic tobacco. *Planta* **195,** 88–97.

Cescatti A. & Niinemets U. (2004) Sunlight capture. Leaf to landscape. In *Photosynthetic Adaptation. Chloroplast to Landscape* (eds W.K. Smith, T.C. Vogelmann & C. Chritchley), pp. 42–85. Springer-Verlag, New York, USA.

Comins H.N. & Farquhar G.D. (1982) Stomatal regulation and water economy in Crassulacean acid metabolism plants: an optimisation model. *Journal of Theoretical Biology* **99,** 263–284.

Cowan I.R. (1977) Stomatal behaviour and environment. *Advances in Botanical Research* **4,** 117–228.

Cowan I.R. (1986) Economics of carbon fixation in higher plants. In *On the Economy of Plant Form and Function* (ed. T.J. Givnish), pp. 133–170. Cambridge University Press, Cambridge, UK.

Cowan I.R. & Farquhar G.D. (1977) Stomatal function in relation to leaf metabolism and environment. *Symposium of the Society for Experimental Biology* **31,** 471–505.

Delzon S., Sartore M., Burlett R., Dewar R. & Loustau D. (2004) Hydraulic responses to height growth in maritime pine trees. *Plant, Cell & Environment* **27,** 1077–1087.

Dewar R.C., Tarvainen L., Parker K., Wallin G. & McMurtrie R.E. (2012) Why does leaf nitrogen decline within tree canopies less rapidly than light? An explanation from optimization subject to a lower bound on leaf mass per area. *Tree Physiology* **32,** 520–534.

Evans J.R. (1987) The relationship between electron transport components and photosynthetic capacity in pea leaves grown at different irradiances. *Australian Journal of Plant Physiology* **14,** 157–170.

Evans J.R. (1989) Partitioning of nitrogen between and within leaves grown under different irradiances. *Australian Journal of Plant Physiology* **16,** 533–548.

Evans J.R. (1993) Photosynthetic acclimation and nitrogen partitioning within a lucerne canopy. II. Stability through time and comparison with a theoretical optimum. *Australian Journal of Plant Physiology* **20,** 69–82.

Evans J.R. (1998) Photosynthetic characteristics of fast- and slow-growing species. In *Inherent Variation in Plant Growth. Physiological Mechanisms and Ecological Consequences* (eds H. Lambers, H. Poorter & M.M.I. Van Vuuren), pp. 101–119. Backhuys Publishers, Leiden, the Netherlands.

Ewers B.E., Oren R., Phillips N., Strömgren M. & Linder S. (2001) Mean canopy stomatal conductance responses to water and nutrient availabilities in *Picea abies* and *Pinus taeda*. *Tree Physiology* **21,** 841–850.

Farquhar G.D. (1989) Models of integrated photosynthesis of cells and leaves. *Philosophical Transactions of the Royal Society of London, Series B* **323,** 357–367.

Farquhar G.D. & Wong S.C. (1984) An empirical model of stomatal conductance. *Australian Journal of Plant Physiology* **11,** 191–210.

Farquhar G.D., von Caemmerer S. & Berry J.A. (1980) A biochemical model of photosynthetic CO_2 assimilation in leaves of C_3 species. *Planta* **149,** 78–90.

Farquhar G.D., Buckley T.N. & Miller J.M. (2002) Stomatal control in relation to leaf area and nitrogen content. *Silva Fennica* **36,** 625–637.

Field C. (1983a) Allocating leaf nitrogen for the maximization of carbon gain: leaf age as a control on the allocation program. *Oecologia* **56,** 341–347.

Field C., Merino J. & Mooney H.A. (1983) Compromises between water-use efficiency and nitrogen-use efficiency in five species of California evergreens. *Oecologia* **60,** 384–389.

Field C.B. (1983b) Allocating nitrogen for the maximization of carbon gain: leaf age as a control on the allocation program. *Oecologia* **56,** 341–347.

Flexas J., Ribas-Carbó M., Diaz-Espejo A., Galmés J. & Medrano H. (2008) Mesophyll conductance to CO_2: current knowledge and future prospects. *Plant, Cell & Environment* **31,** 602–621.

Flexas J., Barbour M.M., Brendel O., *et al*. (2012) Mesophyll diffusion conductance to CO_2: an unappreciated central player in photosynthesis. *Plant Science* **193–194,** 70–84.

Frak E., Le Roux X., Millard P., Adam B., Dreyer E., Escuit C., Sinoquet H., Vandame M. & Varlet-Grancher C. (2002) Spatial distribution of leaf nitrogen and photosynthetic capacity within the foliage of individual trees: disentangling the effects of local light quality, leaf irradiance, and transpiration. *Journal of Experimental Botany* **53,** 2207–2216.

Franks P.J. (2004) Stomatal control of hydraulic conductance, with special reference to tall trees. *Tree Physiology* **24,** 865–878.

Friend A.D. (2001) Modelling canopy CO_2 fluxes: are 'big-leaf' simplifications justified? *Global Ecology and Biogeography* **10,** 603–619.

Gonzales-Real M.M. & Baille A. (2000) Changes in leaf photosynthetic parameters with leaf position and nitrogen content within a rose plant canopy (*Rosa hybrida*). *Plant, Cell & Environment* **23,** 351–363.

Gutschick V.P. & Wiegel F.W. (1988) Optimizing the canopy photosynthetic rate by patterns of investment in specific leaf mass. *The American Naturalist* **132,** 67–86.

Haefner J.W., Buckley T.N. & Mott K.A. (1997) A spatially explicit model of patchy stomatal responses to humidity. *Plant, Cell & Environment* **20,** 1087–1097.

Hikosaka K. & Terashima I. (1995) A model of the acclimation of photosynthesis in the leaves of C3 plants to sun and shade with respect to nitrogen use. *Plant, Cell & Environment* **18,** 605–618.

Hikosaka K. & Terashima I. (1996) Nitrogen partitioning among photosynthetic components and its consequence in sun and shade plants. *Functional Ecology* **10,** 335–343.

Hirose T. & Werger M.J.A. (1987) Maximizing daily canopy photosynthesis with respect to the leaf nitrogen allocation pattern in the canopy. *Oecologia* **72,** 520–526.

Hirose T. & Werger M.J.A. (1994) Photosynthetic capacity and nitrogen partitioning among species in the canopy of a herbaceous plant community. *Oecologia* **100,** 203–212.

Hollinger D.Y. (1996) Optimality and nitrogen allocation in a tree canopy. *Tree Physiology* **16,** 627–634.

Hubbard R.M., Bond B.J. & Ryan M.G. (1999) Evidence that hydraulic conductance limits photosynthesis in old *Pinus ponderosa* trees. *Tree Physiology* **19,** 165–172.

Jones H.G. (1992) *Plants and Microclimate* 2nd edn, Cambridge University Press, Cambridge.

June T., Evans J.R. & Farquhar G.D. (2004) A simple new equation for the reversible temperature dependence of photosynthetic electron transport: a study on soybean leaf. *Functional Plant Biology* **31,** 275–283.

Koch G.W., Sillett S.C., Jennings G.M. & Davis S.D. (2004) The limits to tree height. *Nature* **42,** 851–854.

Kull O. (2002) Acclimation of photosynthesis in canopies: models and limitations. *Oecologia* **133,** 267–279.

Kull O. & Kruijt B. (1998) Leaf photosynthetic light response: a mechanistic model for scaling photosynthesis to leaves and canopies. *Functional Ecology* **12,** 767–777.

Le Roux X., Bariac T., Sinoquet H., Genty B., Piel C., Mariotti A., Girardin C. & Richard P. (2001) Spatial distribution of leaf water-use efficiency and carbon isotope discrimination within an isolated tree crown. *Plant, Cell & Environment* **24,** 1021–1032.

Leuning R., Kelliher F.M., de Pury D.G.G. & Schulze E.D. (1995) Leaf nitrogen, photosynthesis, conductance and transpiration: scaling from leaves to canopies. *Plant, Cell & Environment* **18,** 1183–1200.

Lloyd J., Patino S., Paiva R.Q., *et al*. (2010) Optimisation of photosynthetic carbon gain and within-canopy gradients of associated foliar traits for Amazon forest trees. *Biogeosciences* **7,** 1833–1859.

Makino A., Sato T., Nakano H. & Mae T. (1997) Leaf photosynthesis, plant growth and nitrogen allocation in rice under difference irradiances. *Planta* **203,** 390–398.

Miller J.M. (2002) *Carbon Isotope Discrimination by Eucalyptus Species*. The Australian National University, Canberra, Australia.

Miller J.M., Williams R.J. & Farquhar G.D. (2001) Carbon isotope discrimination by a sequence of Eucalyptus species along a sub-continental rainfall gradient in Australia. *Functional Ecology* **15,** 222–232.

Niinemets U. (2012) Optimization of foliage photosynthetic capacity in tree canopies: towards identifying missing constraints. *Tree Physiology* **32,** 505–509.

Niinemets Ü., Cescatti A., Rodeghiero M. & Tosens T. (2005) Leaf internal diffusion conductance limits photosynthesis more strongly in older leaves of Mediterranean evergreen broad-leaved species. *Plant, Cell & Environment* **28,** 1552–1566.

Niinemets Ü., Cescatti A., Rodeghiero M. & Tosens T. (2006) Complex adjustments of photosynthetic potentials and internal diffusion conductance to current and previous light availabilities and leaf age in Mediterranean evergreen species *Quercus ilex*. *Plant, Cell & Environment* **29,** 1159–1178.

Ögren E. & Evans J.R. (1993) Photosynthetic light response curves. I. The influence of CO_2 partial pressure and leaf inversion. *Planta* **189,** 182–190.

Oren R., Sperry J.S., Katul G.G., Pataki D.E., Ewers B.E., Phillips N. & Schafer K.V.R. (1999) Survey and synthesis of intra- and interspecific variation in stomatal sensitivity to vapour pressure deficit. *Plant, Cell & Environment* **22,** 1515–1526.

Oren R., Sperry J.S., Ewers B.E., Pataki D.E., Phillips N. & Megonigal J.P. (2001) Sensitivity of mean canopy stomatal conductance to vapor pressure deficit in a flooded *Taxodium distichum* L. forest: hydraulic and non-hydraulic effects. *Oecologia* **126,** 21–29.

Pearcy R.W. (1990) Sunflecks and photosynthesis in plant canopies. *Annual Review of Plant Physiology* **41,** 421–453.

Peisker M. (1973) CO2-Aufnahme, Transpiration und Blattemperatur unter dem EinfluB yon Anderungen der Stomataweite. *Kulturpflanze* **21,** 97–109.

Peltoniemi M.S., Duursma R.A. & Medlyn B.E. (2012) Co-optimal distribution of leaf nitrogen and hydraulic conductance in plant canopies. *Tree Physiology* **32,** 510–519.

Phillips N., Bond B.J., McDowell N.G. & Ryan M.G. (2002) Canopy and hydraulic conductance in young, mature and old Douglas-fir trees. *Tree Physiology* **22,** 205–211.

Pons T.L. & Pearcy R.W. (1994) Nitrogen reallocation and photosynthetic acclimation in response to partial shading in soybean plants. *Physiologia Plantarum* **92,** 636–644.

Press W.H., Teukolsky S.A., Vetterling W.T. & Flannery B.P. (1992) *Numerical Recipes in C++: The Art of Scientific Computing* 2nd edn, Cambridge University Press, Cambridge, UK.

de Pury D.G.G. & Farquhar G.D. (1997) Simple scaling of photosynthesis from leaves to canopies without the errors of big-leaf models. *Plant, Cell & Environment* **20,** 537–557.

Roderick M.L. (1999) Estimating the diffuse component from daily and monthly measurements of global radiation. *Agricultural and Forest Meteorology* **95,** 169–185.

Ryan M.G., Bond B.J., Law B.E., Hubbard R.M., Woodruff D., Cienciala E. & Kucera J. (2000) Transpiration and whole-tree conductance in ponderosa pine trees of different heights. *Oecologia* **124,** 553–560.

Ryan M.G., Phillips N. & Bond B.J. (2006) The hydraulic limitation hypothesis revisited. *Plant, Cell & Environment* **29,** 367–381.

Sands P.J. (1995) Modelling canopy production. I. Optimal distribution of photosynthetic resources. *Australian Journal of Plant Physiology* **22,** 593–601.

Schieving F. & Poorter H. (1999) Carbon gain in a multispecies canopy: the role of specific leaf area and photosynthetic nitrogen-use efficiency in the tragedy of the commons. *New Phytologist* **143,** 201–211.

Schulze E.D., Williams R.J., Farquhar G.D., Schulze W., Langridge J., Miller J.M. & Walker B.H. (1998) Carbon and nitrogen isotope discrimination and nitrogen nutrition of trees along a rainfall gradient in northern Australia. *Australian Journal of Plant Physiology* **25,** 413–425.

Sellers P.J., Berry J.A., Collatz G.J., Field C.B. & Hall F.G. (1992) Canopy reflectance, photosynthesis and transpiration. III: a reanalysis using improved leaf models and a new canopy integration scheme. *Remote Sensing of the Environment* **42,** 187–216.

Terashima I. & Evans J.R. (1988) Effects of light and nitrogen nutrition on the organization of the photosynthetic apparatus in spinach. *Plant and Cell Physiology* **29,** 143–155.

Terashima I. & Hikosaka K. (1995a) Comparative ecophysiology of leaf and canopy photosynthesis. *Plant, Cell & Environment* **18,** 1111–1128.

Terashima I. & Hikosaka K. (1995b) Comparative ecophysiology of leaf and canopy photosynthesis. *Plant, Cell & Environment* **18,** 1111–1128.

Terashima I. & Inoue Y. (1984) Comparative photosynthetic properties of palisade tissue chloroplasts and spongy tissue chloroplasts of *Camellia japonica* L.: functional adjustment of photosynthetic apparatus to light environment within a leaf. *Plant and Cell Physiology* **25,** 555–563.

Warren C.R. (2007) Stand aside stomata, another actor deserves centre stage: the forgotten role of the internal conductance to CO_2 transfer. *Journal of Experimental Botany* **59,** 1475–1487.

Warren C.R. & Adams M.A. (2006) Internal conductance does not scale with photosynthetic capacity: implications for carbon isotope discrimination and the economics of water and nitrogen use in photosynthesis. *Plant, Cell & Environment* **29,** 192–201.

Yoder B.J., Ryan M.G., Waring R.H., Schoettle A.W. & Kaufmann M.R. (1994) Evidence of reduced photosynthetic rates in old trees. *Forest Science* **40,** 513–527.

Received 5 November 2012; accepted for publication 1 March 2013

APPENDIX

We used a process-based model of leaf gas exchange, in which key resource-dependent physiological parameters are determined for each leaf by numerical optimization. These parameters are maximum RuBP carboxylation velocity at 25 °C (V_{m25}), maximum potential electron transport rate at 25 °C (J_{m25}), leaf absorptance to photosynthetically active light (α) and the diurnal time course of stomatal conductance to water vapour [$g_{sw}(t)$] (variables and symbols are defined in Table 1).

Leaf gas exchange model

In the biochemical photosynthesis model of Farquhar *et al.* (1980), the net assimilation rate (A) at any given chloroplastic CO_2 concentration (c_c) is the lesser of two rates: a RuBP carboxylation-limited rate (A_{Dv}) and a RuBP regeneration-limited rate (A_{Dj}):

$$A_{Dv} = \frac{V_m(c_c - \Gamma_*)}{c_c + K_c(1 + O/K_o)} - R_d \quad \text{(A1)}$$

and

$$A_{Dj} = \frac{J}{4}\frac{(c_c - \Gamma_*)}{(c_c + 2\Gamma_*)} - R_d, \quad \text{(A2)}$$

where V_m is the maximum RuBP carboxylation velocity, Γ_* is the photorespiratory CO_2 compensation point, K_c is the Michaelis constant for RuBP carboxylation, O is the concentration of O_2, K_o is the Michaelis constant for RuBP oxygenation, R_d is the rate of non-photorespiratory CO_2 release in the light and J is the potential electron transport rate. We assumed $R_{d25} = 0.0089 \cdot V_{m25}$ (de Pury & Farquhar 1997). The simple minimum of A_{Dv} and A_{Dj} is not differentiable at the transition between carboxylation and regeneration limitation, which presents a challenge for numerical optimization. We addressed this by calculating A_D as the hyperbolic minimum (Eqn A3) of the two limiting rates, which 'smooths' the transition:

$$A_D = \text{minh}\{A_{Dv}, A_{Dj}, \theta_A\}, \quad \text{(A3)}$$

where minh$\{x,y,\theta\}$ is defined as the lesser root z of $\theta z^2 - (x + y)z + xy = 0$ and $\theta < 1$. [Note that Eqns A1–A3 are identical to the original model of Farquhar *et al.* (1980) when c_c is above the CO_2 compensation point, but not below. This distinction is immaterial in our model because it only applies when $A < 0$, a situation that cannot occur in our model because it would cause $\partial A/\partial E$ to become negative. Assimilation is also limited by CO_2 diffusion from the atmosphere to the sites of carboxylation (A_s):

$$A_s = \frac{c_a - c_c}{g_{bc}^{-1} + g_{sc}^{-1} + g_m^{-1}}, \quad \text{(A4)}$$

where c_a is the ambient CO_2 concentration, g_{bc} is the boundary layer conductance to CO_2 (discussed below under the section *Leaf temperature*), g_{sc} is the stomatal conductance to CO_2 ($g_{sc} = 1.6 \cdot g_{sw}$, where g_{sw} is the stomatal conductance to H_2O (discussed below under the section *Numerical optimization procedures*)) and g_m is mesophyll conductance to CO_2 (discussed below under the section *Mesophyll conductance*). The actual value of A is then the intersection of A_D and A_s:

$$A = A_s \cap A_D. \quad \text{(A5)}$$

Leaf transpiration rate, E, was computed as

$$E = g_{tw}(w_{sl} - w_a)/(1 - 0.5(w_{sl} + w_a)) \quad \text{(A6)}$$

(von Caemmerer & Farquhar 1981), where g_{tw} is the total conductance to water vapour, w_{sl} (mol mol^{-1}) is the saturation water vapour mole fraction at the leaf temperature T_l, and w_a is the water vapour mole fraction of the air. $g_{tw} = g_{sw} \cdot g_{bw}/(g_{sw} + g_{bw})$, where g_{sw} and g_{bw} are stomatal and boundary layer conductances to water vapour, respectively. g_{sw} was numerically optimized (see the section *Numerical optimization procedures*); computation of g_{bw} is discussed under the section *Leaf temperature*.

Modelling potential electron transport rate and light capture

Potential electron transport rate, J, has traditionally been modelled as a saturating function of total irradiance, I, and maximum potential electron transport rate, J_m. A common form for this relationship is the hyperbolic minimum of J_m and J_i: $J = \text{minh}\{J_m, J_i, \theta_j\}$, where minh$\{x, y, \theta\}$ is defined in the text below Eqn A3, $J_i = \alpha I(1 - F)/2$, α is the leaf absorptance, F (0.23; Farquhar & Wong 1984) is the fraction of photons that are absorbed but do not lead to photo-oxidation of water, the 1/2 factor accounts for the two photosystems and $\theta_j < 1$ is a curvature factor. Because this model does not distinguish between photons received at the upper and lower surfaces of

broad leaves, nor between leaves with different transdermal profiles of photosynthetic capacity, it precludes rigorous assessment of the roles of light capture and varying transdermal irradiance regime in N optimization. We therefore used the *J* model of Buckley & Farquhar (2004), which treats upper and lower surface irradiances separately and explicitly simulates the transdermal profile of electron transport capacity as a weighted average of exponential profiles declining from either leaf surface. In this study, we assumed that the weighting for the upper surface (w_u) is equal to the time-averaged fraction of total leaf irradiance received at that surface (the weight for the lower surface is the complement of w_u, $1 - w_u$). This captures the tendency for the transdermal capacity profile to adapt to irradiance regime (Ögren & Evans 1993). The model is

$$J = \text{minh}\{J_i - J_s, J_m + J_s, \theta_j\}, \tag{A7}$$

where J_s is related to the amount of excess light absorbed by light-saturated transdermal layers when some other layers are light-limited, and is given by $J_s = \max\{0, J_{su}, J_{sl}\}$, where

$$\begin{aligned} J_{su} &= \left(\frac{\alpha F I_u - w_u J_m}{1-\tau}\right)\left(1 - \sqrt{\tau\frac{\alpha F I_u - w_u J_m}{\alpha F I_l - (1-w_u)J_m}}\right)^2 \\ J_{sl} &= \left(\frac{\alpha F I_l - (1-w_u)J_m}{1-\tau}\right)\left(1 - \sqrt{\tau\frac{\alpha F I_l - (1-w_u)J_m}{\alpha F I_u - w_u J_m}}\right)^2 \end{aligned} \tag{A8}$$

and I_u and I_l are the irradiances at the upper and lower leaf surfaces, respectively, τ is leaf transmissivity to non-reflected light and α is the leaf absorptance. α is calculated from leaf chlorophyll content (Eqn A17), which, in turn, depends on N allocation, as discussed below. τ is calculated as $\exp(-3.9\cdot[\text{Chl}])$, where [Chl] is the leaf chlorophyll content (mmol m^{-2}) (Eqn A18 below). Full derivation of this model is given in Buckley & Farquhar (2004).

Modelling the crown light environment

The light regime of an artificial, horizontally uniform canopy composed of flat circular leaves was estimated using ray-tracing. This allows direct numerical simulation of irradiance at the leaf scale, by accounting for the spatial-angular arrangement and optical properties of individual leaves. The canopy was built with 8000 randomly located Lambertian leaves, characterized by a spherical angular distribution. The crown height was 5 m, the leaf radius was 6 cm and the LAI was 4 m^2 m^{-2}. In the computation of the leaf beam irradiance, the condition of penumbra generated by the partial obstruction of the solar disk was simulated according to Cescatti & Niinemets (2004). One thousand rays were fired from each leaf in the direction of the sun disk and the fraction of the sun visible from the leaf surface was computed. Un-intercepted diffuse light irradiance was estimated by firing 1000 rays from the sky hemisphere to each leaf, assuming a standard overcast sky distribution of the incoming radiation. Fluxes of radiation scattered by phytoelements and soil were computed assuming a Lambertian behaviour of the surfaces. Finally, the relative beam and diffuse irradiance (including scattered fluxes) were calculated separately for each side of each leaf. This was repeated at different solar angles (in 3 degree intervals). The actual irradiance at each leaf surface were calculated as the product of the above crown beam and diffuse incoming irradiance and the relative beam and diffuse leaf irradiance.

The photosynthesis model used total upper and lower surface irradiances ($I_u = I_{du} + I_{bu}$, $I_l = I_{dl} + I_{bl}$), where d and b denote diffuse and beam irradiances, respectively, and u and l denote upper and lower leaf surfaces, respectively. These irradiances were computed as fractions of above-crown values (I_{od}, I_{ob}) by ray-tracing, as described earlier. The above-crown diffuse and beam irradiances were computed as $I_{od} = f_d I_{og}$ and $I_{ob} = I_{og} - I_{od}$, respectively, where I_{og} is the global irradiance (photosynthetic photon flux density) and f_d is the diffuse fraction of daily above-crown global irradiance. f_d was computed following Roderick (1999):

$$f_d = \begin{cases} Y_0 & K \le X_0 \\ A_0 + A_1 K \quad if & X_0 < K \le X_1 \\ Y_1 & K > X_1 \end{cases} \tag{A9}$$

where $X_0 = 0.26$, $X_1 = 0.80 - 0.0017|lat| + 0.000044\cdot lat^2$ (*lat* is latitude in degrees; $lat = -30^\circ$ for the simulations shown here), $Y_0 = 0.96$, $Y_1 = 0.05$, $A_0 = Y_1 - A_1 X_1$, $A_1 = (Y_1 - Y_0)/(X_1 - X_0)$, and K is the ratio of daily global irradiance to that above the atmosphere, given by

$$K = 0.23 + 0.50 p_{sun} \tag{A10}$$

(Roderick 1999). At each point in time, we computed gas exchange under two conditions – sunny and cloudy – and weighted the resulting values by p_{sun} (the ratio of sunshine hours to total daytime hours, or the instantaneous probability of sunshine) and its complement, respectively. Under cloudy conditions, $I_{og} = 0.23 I_o$ and under sunny conditions $I_{og} = 0.73 I_o$, where I_o is the global irradiance (photosynthetic photon flux density) above the atmosphere. I_o equals $I_{o,max}\sin\beta$, where $I_{o,max}$ (μmol m^{-2} s^{-1}) $= 2413[1 + 0.033\cos(2\pi J_{day}/365)]$ (Leuning *et al*. 1995), J_{day} is day of year (January 1 = 0; $J_{day} = 0$ for the simulations shown here) and β is the solar elevation angle.

Because crown light penetration was computed at equal intervals of β, time (t, hours) was computed from β rather than the reverse: $t(\beta) = 12(1 - \arccos((\sin\beta - a)/b))$, where $a = \sin(lat\ \pi/180)\cdot\sin\delta$, $b = \cos(lat\ \pi/180)\cos\delta$ and $\delta = -23.4(\pi/180)\cos[2\pi(J_{day} + 10)/365]$ (Leuning *et al*. 1995; de Pury & Farquhar 1997). Time step size (δt, hours) was estimated as the product of the solar angle step size ($\delta\beta = \pi/60$) and the derivative of $t(\beta)$ with respect to β:

$$\delta t = \cos\beta \Big/ 5\sqrt{b^2 - (\sin\beta - a)^2}\,. \tag{A11}$$

Daily totals for irradiance and gas exchange variables were then computed by summing the products of their respective instantaneous values and δt at each value of β.

Leaf temperature

The parameters V_m, J_m, $\Gamma*$, K_c, K_o and R_d were calculated from their values at 25 °C (indicated by the subscript '25')

using temperature responses given by June, Evans & Farquhar (2004) for J_m and by Bernacchi *et al.* (2001) for the other parameters. Leaf temperature (T_l) was determined using the following approximation, which arises by expanding $T_l^4 - T_a^4$ in terms of $\Delta T = (T_l - T_a)$ and ignoring second-order or higher terms in ΔT, and by approximating the saturation vapour pressure versus temperature curve with a line segment (e.g. Peisker 1973; Jones 1992):

$$T_l = T_a + \frac{\Phi + f_{ir}(\varepsilon_a - 1)\sigma T_{aK}^4 - l g_{tw} D_{air}}{4 f_{ir}\sigma T_a^3 + 2 c_p g_{bh} + l g_{tw} s}. \quad \text{(A12)}$$

In Eqn A12, Φ is the shortwave radiation, f_{ir} is the fraction of infrared radiation from the sky visible at this point in the crown, ε_a is the atmospheric IR emissivity, σ (5.67×10^{-8} J m^{-2} s^{-1} K^{-4}) is the Stefan–Boltzmann constant, T_{aK} is the air temperature in Kelvins, l is the latent heat of vaporization, D_{air} is the vapour mole fraction deficit of the air, c_p is the molar heat capacity of air, g_{bh} is boundary layer conductance to heat and s is the slope of the saturation H_2O vapour mole fraction versus temperature curve. Φ (J m^{-2} s^{-1}) was computed as $0.5666(I_u + I_l)$, based on the ratio of extraterrestrial quantum flux (2413 μmol m^{-2} s^{-1}) to energy flux (1367 J m^{-2} s^{-1}) (de Pury & Farquhar 1997). To compute f_{ir}, we assumed that IR penetrated the crown with the same extinction coefficient as diffuse visible irradiance, so f_{ir} (unitless) = $(I_{du} + I_{dl})/I_{od}$. ε_a was computed as $(10^5\ w_a/T_{aK})$ (Leuning *et al.* 1995); 10^5 converts units of w_a (mol mol^{-1}) to Pa, assuming atmospheric pressure of 100 kPa. l (J mol^{-1}) = 18.01·(2501 – T_l·0.002378). D_{air} (mol mol^{-1}) = $w_{sa} - w_a$, where w_{sa} is the saturation mole fraction at air temperature T_a. c_p (J mol^{-1} K^{-1}) = 29.25. The slope of w_s versus T, s (mol mol^{-1} K^{-1}) at T_a is w_{sa}·0.0173·237.3/$(T_a + 237.3)^2$. g_{bh} (mol m^{-2} s^{-1}) was computed as the sum of terms representing forced (g_{bhw}) and free convection (g_{bhf}). The former is

$$g_{bhw} = 0.123\sqrt{v/w}, \quad \text{(A13)}$$

where w is downwind leaf width (m) and v (m s^{-1}) is the wind speed, which we assumed declines exponentially in the crown in the same fashion as diffuse irradiance, so $v = f_{ir}\cdot v_o$, where v_o is the wind speed above the crown. Conductance for free convection, g_{bhf}, is

$$g_{bhf} = 0.5(\kappa/c_p w)\cdot(1.6\times10^8 |T_l - T_a| w^3)^{0.25}, \quad \text{(A14)}$$

where κ (J s^{-1} m^{-1} K^{-1}) is the thermal conductivity of air $[0.026 + 5.6 \times 10^{-5}(T_a - 20)]$, and the quantity raised to the 0.25 power at right is the Grashof number (dimensionless). Because T_l depends on g_{bhf} (cf. Eqns A12 and A14), we computed an initial estimate of T_l using $g_{bhf} = 0$, applied this to Eqn A14 to compute g_{bhf} and recalculated T_l with Eqn A12; we then repeated this cycle one more time. Subsequent iterations produced negligible changes in leaf temperature. Boundary layer conductance to water vapour, g_{bw}, was computed as $1.08 g_{bh}$, and boundary layer conductance to CO_2, g_{bc}, was $1.37 g_{bw}$.

Mesophyll conductance

The conductance to CO_2 transfer from the intercellular spaces to the sites of carboxylation, termed mesophyll conductance (g_m), varies greatly among species and in relation to photosynthetic capacity (e.g. Warren 2007). Because the physical nature of g_m remains poorly understood, it is not yet possible to calculate g_m from known biophysical parameters, so we specified g_m by using two alternative assumptions. The default assumption was that g_m is proportional to V_{m25}, that is, that it scales linearly and homogeneously with photosynthetic capacity: g_m/(mol m^{-2} s^{-1}) = $0.004 V_{m25}$/(μmol m^{-2} s^{-1}). The slope of 0.004 was taken from the relationship among estimates of g_m and V_{m25} by Warren & Adams (2006). The alternative assumption was that g_m is constant and is independent of photosynthetic capacity; in that scenario, g_m was set at 0.34 mol m^{-2} s^{-1}, the assimilation-weighted mean from the default simulation. These two alternatives should be viewed as limiting cases.

Numerical optimization procedures

The outer N loop and the stomatal conductance optimization loop both used the golden search method, initiated by triplet bracketing of the solution (Press *et al.* 1992), to identify the values of leaf photosynthetic N or g_{sw} for which $\partial N/\partial A_d$ and $\partial E/\partial A$ equalled the imposed 'target' values (ν and λ, respectively). The inner N loop, which partitioned total N among functional pools, used a Nelder–Mead downhill simplex to identify the optimal partitioning vector (f_v, f_j, f_c, the fractions of N invested in carboxylation, electron transport and light capture, respectively; see below for more details). Implementing a simplex algorithm in the finite space defined by complementary allocation fractions (in this example, the space is the triangular plane fragment formed by bounding the plane $1 = f_v + f_j + f_c$ between 0 and 1 for each allocation fraction), is difficult because the simplex can jump out of this space. Thus, in our simulations, the simplex searched an infinite two-dimensional space defined by log ratio transformation of the allocation fractions; thus, $x = \ln(f_v/f_j)$ and $y = \ln(f_v/f_c)$. x and y coordinates of simplex vertices in this space were transformed back to f_v, f_j and f_c as follows: $f_c = 1/(1 + e^y + e^{y-x})$, $f_j = f_c e^{y-x}$ and $f_v = f_c e^y$.

Computing photosynthetic parameters from N pools

Our treatment of functional nitrogen economy was derived from that presented by Hikosaka & Terashima (1995), who considered five N pools or 'groups'. Group I is N in Rubisco; group II is N in the electron transport chain [excluding photosystems I and II (PSI and PSII, respectively)], coupling factor and Calvin cycle enzymes other than Rubisco; group III is N in the PSII core; group IV is N in the PSI core, combined with light-harvesting complex I (LHCI); and group V is N in light-harvesting complex II (LHCII).

We re-organized these groups into three functional pools: pool 'V' (denoted as N_v) is simply group I from Hikosaka & Terashima (1995) and represents investment in carboxylation capacity. Pool 'J' (denoted as N_j) is groups II and III combined, and represents investment in electron transport capacity. Pool 'C' (denoted as N_c) is groups IV and V combined, and represents investment in light capture. These pools are related to photosynthetic parameters as follows:

$$V_{m25} = \chi_v N_v, \tag{A15}$$

$$J_{m25} = \chi_j N_j, \tag{A16}$$

and

$$\alpha = [\text{Chl}]/([\text{Chl}] + 0.076), \tag{A17}$$

where

$$[\text{Chl}] = \chi_{cj} N_j + \chi_c N_c. \tag{A18}$$

In Eqns A17 and A18, [Chl] is the leaf chlorophyll content and the χ terms are nitrogen costing coefficients, as discussed below. The expression for leaf absorptance (α) was given by Evans (1998). The expression for [Chl] reflects the fact that group III, which is part of N_j in our treatment, includes chlorophyll binding proteins that are covalently bound to the PSII core. Thus, allocation to electron transport capacity and light capture are not fully separable. We estimated the nitrogen costing coefficients (χ_v, χ_j, χ_{jc}, χ_c) as follows.

(a) χ_v: There are 6290 mol N mol^{-1} Rubisco molecules (Hikosaka & Terashima 1995) and 8 active sites per molecule. Assuming a turnover rate of 3.53 s^{-1} (von Caemmerer *et al*. 1994), this gives (3.53 mol CO_2 s^{-1} site^{-1}) (8 mol sites-mol^{-1} Rubisco)/(6290 mol N mol^{-1} Rubisco) = 0.004490 mol CO_2 s^{-1} mol^{-1} N, or χ_v = 4.49 μmol CO_2 s^{-1} mmol^{-1} N.

(b) χ_j: In our treatment, $N_j = N_{II} + N_{III}$, Hikosaka & Terashima (1995) gave functional dependences of maximum photosynthetic rate (P_{max}) on the concentrations of cytochrome *f* ([cyt *f*]) and PSII ([PSII]), which they took as representative of Groups II and III: $P_{max} = a_f$[cyt *f*] = a_p[PSII]. This implies a stoichiometric constraint between Groups II and III: [PSII] = (a_f/a_p)[cyt *f*]. Denoting the N costs of groups II and III as χ_{II} and χ_{III}, respectively, this yields ($\chi_{III}N_{III}$) = (a_f/a_p)($\chi_{II}N_{II}$) or (N_{III}/N_{II}) = (a_f/a_p)(χ_{II}/χ_{III}). Thus, $NII + N_{III}$ = N_{II}(1 + (a_f/a_p)(χ_{III}/χ_{II})), or in terms of N_j,

$$N_j = N_{II} + N_{III} = N_{II}(1 + a_f\chi_{II}/a_p\chi_{III}). \tag{A19}$$

In Hikosaka & Terashima (1995), P_{max} equalled 0.56 times the rate of O_2 evolution at saturating CO_2 and light. The latter rate is $J_m/4$, so $P_{max} = 0.56J_m/4$. From above, $P_{max} = a_f$[cyt *f*] = $a_f\chi_{II}N_{II}$. Combining these expressions for P_{max} and solving for N_{II} gives $N_{II} = (0.56/4)J_m/(a_f\chi_{II})$. Replacing J_m with $\chi_j N_j$ and applying this to Eqn A19 gives

$$N_j = \chi_j N_j \frac{0.56}{4a_f\chi_{II}}\left(1 + \frac{a_f\chi_{II}}{a_p\chi_{III}}\right), \tag{A20}$$

which is solved for χ_j:

$$\chi_j = \frac{4a_f a_p \chi_{II}\chi_{III}}{0.56(a_f\chi_{II} + a_p\chi_{III})}. \tag{A21}$$

From Hikosaka & Terashima (1995), χ_{II} and χ_{III} are 9530 mol N mol^{-1} cyt *f* and 5000 mol N mol^{-1} PSII, respectively, and a_f and a_s are 19.9 mol s^{-1} mol^{-1} and 0.00174 mol mol^{-1}, respectively, giving χ_j = 0.009478 mol e$^-$ s^{-1} mol^{-1} N or χ_j = 9.478 μmol e$^-$ s^{-1} mmol^{-1} N.

(c) χ_{jc} and χ_c: Chlorophyll is associated with Hikosaka & Terashima's (1995) groups III, IV and IV such that

$$[\text{Chl}] = \chi_{cIII}N_{III} + \chi_{cIV}N_{IV} + \chi_{cV}N_V, \tag{A22}$$

where χ_{cIII}, χ_{cIV} and χ_{cV} are the molar ratios of N/binding Chl in froups III, IV and V, respectively. In our treatment, $N_c = N_{IV} + N_V$. From above, $N_{III} = N_{II}(a_f\chi_{II}/a_p\chi_{III})$ and $N_j = N_{II}(1 + a_f\chi_{II}/a_p\chi_{III})$. Thus, $N_{III} = N_j a_f\chi_{II}/(a_f\chi_{II} + a_p\chi_{III})$, which applied to Eqn A22 gives

$$[\text{Chl}] = \left(\frac{a_f\chi_{II}\chi_{cIII}}{a_f\chi_{II} + a_p\chi_{III}}\right)N_j + \chi_{cIV}N_{IV} + \chi_{cV}N_V. \tag{A23}$$

The first term in parentheses is thus χ_{cj}, from Eqn A18. From Hikosaka & Terashima (1995), χ_{cIII} is 1/83.3, giving $\chi_{cj} = 4.64 \times 10^{-4}$ mol Chl mol^{-1} N. Inspection of Eqns A18 and A23 shows

$$\chi_c(N_{IV} + N_V) = \chi_{cIV}N_{IV} + \chi_{cV}N_V, \tag{A24}$$

which can be rearranged to give χ_c as

$$\chi_c = \frac{\chi_{cIV} + \chi_{cV}(N_V/N_{IV})}{1 + (N_V/N_{IV})}. \tag{A25}$$

Thus, χ_c is a function of N_V/N_{IV}. This equation can be solved for the ratio N_V/N_{IV}:

$$\frac{N_V}{N_{IV}} = \frac{1}{\chi_{cV}}\left(\frac{[\text{Chl}]}{N_{IV}} - \chi_{cj}\frac{N_j}{N_{IV}} - \chi_{cIV}\right). \tag{A26}$$

To simplify further, we adopt Hikosaka & Terashima's (1995) assumption that [Chl] is proportional to [PSI] (and thus to N_{IV}). This leads to [PSII] = a_s[Chl], where a_s is a proportionality constant. By definition [PSII] = $\chi_{IV}N_{IV}$, so $\chi_{IV}N_{IV}$ = a_s[Chl], allowing [Chl]/N_{IV} in Eqn A26 to be replaced with χ_{IV}/a_s. Likewise, N_{IV} in the denominator of the second term in parentheses in Eqn A26 can be replaced with a_s[Chl]/χ_{IV}, and N_j can be replaced with J_m/χ_j. This gives

$$\frac{N_V}{N_{IV}} = \frac{1}{\chi_{cV}}\left(\frac{\chi_{IV}}{a_s}\left(1 - \frac{\chi_{cj}}{\chi_j}\frac{J_m}{[\text{Chl}]}\right) - \chi_{cIV}\right). \tag{A27}$$

This shows that N_v/N_{IV} depends on the ratio of J_m to leaf Chl content. Evans (1989) found that this ratio varied from 0.264 to 0.356 mol mol^{-1}, averaging 0.305. When this range for N_V/N_{IV} is applied to Eqn A25, using values for the other parameters in Eqn A27 given by Hikosaka & Terashima (1995) or calculated above, the resulting estimates for χ_c range from 0.03337 to 0.03416 and average 0.03384 mol Chl mol^{-1} N. The extremes differ from the average by only ± 2%, so we simply assumed χ_c = 0.03384 mol Chl mol^{-1} N.